



UNIVERSITY OF LEEDS

This is a repository copy of *Optical Frequency Combs for Molecular Spectroscopy, Kinetics, and Sensing*.

White Rose Research Online URL for this paper:

<https://eprints.whiterose.ac.uk/176520/>

Version: Accepted Version

Book Section:

Lehman, J orcid.org/0000-0001-6610-6519 and Weichman, ML (2021) Optical Frequency Combs for Molecular Spectroscopy, Kinetics, and Sensing. In: Emerging Trends in Chemical Applications of Lasers. ACS Symposium Series, 1398 . American Chemical Society , pp. 61-88. ISBN 9780841298040

<https://doi.org/10.1021/bk-2021-1398.ch004>

© 2021 American Chemical Society. This is an author produced version of a book chapter published in Emerging Trends in Chemical Applications of Lasers. Uploaded in accordance with the publisher's self-archiving policy.

Reuse

Items deposited in White Rose Research Online are protected by copyright, with all rights reserved unless indicated otherwise. They may be downloaded and/or printed for private study, or other acts as permitted by national copyright laws. The publisher or other rights holders may allow further reproduction and re-use of the full text version. This is indicated by the licence information on the White Rose Research Online record for the item.

Takedown

If you consider content in White Rose Research Online to be in breach of UK law, please notify us by emailing eprints@whiterose.ac.uk including the URL of the record and the reason for the withdrawal request.



eprints@whiterose.ac.uk
<https://eprints.whiterose.ac.uk/>

This document is confidential and is proprietary to the American Chemical Society and its authors. Do not copy or disclose without written permission. If you have received this item in error, notify the sender and delete all copies.

**Optical Frequency Combs for Molecular Spectroscopy,
Kinetics, and Sensing**

Journal:	<i>ACS Books</i>
Manuscript ID	bk-2021-00183m.R1
Manuscript Type:	Symposium Series Chapter
Date Submitted by the Author:	24-Jun-2021
Complete List of Authors:	Lehman, Julia; University of Leeds, School of Chemistry Weichman, Marissa; Princeton University, Chemistry

SCHOLARONE™
Manuscripts

Optical Frequency Combs for Molecular Spectroscopy, Kinetics, and Sensing

Julia H. Lehman^{1,*} and Marissa L. Weichman^{2,*}

¹School of Chemistry, University of Leeds, Leeds, LS2 9JT, UK

²Department of Chemistry, Princeton University, Princeton, NJ, 08544, USA

*Email: j.lehman@leeds.ac.uk, weichman@princeton.edu

With rapidly developing technological advances and increasing commercialization, optical frequency combs are beginning to see use in chemical laboratories around the world. These light sources allow chemists to collect high-resolution, multiplexed direct absorption spectra in a fraction of the laboratory time required by more conventional methods. Broadband coupling of combs into high-finesse optical cavities continues to break new ground in the sensitivity of both frequency- and time-resolved spectroscopies. Analytical sensing applications are also undergoing a burst of activity as comb systems become miniaturized, turn-key, and more robust in rugged environments. In this Chapter, we introduce frequency comb spectroscopy and survey its recent applications to molecular spectroscopy and dynamics, chemical reaction kinetics, and sensing.

1 Introduction

Optical frequency combs, laser light sources whose frequency-domain spectra consist of a series of narrow evenly spaced lines, have become a robust tool in the arsenal of techniques available to modern physical and analytical chemists. Frequency combs were initially developed through a fruitful marriage of the fields of ultrafast science and precision measurement^{1,2} and enabled direct referencing between radiofrequency (RF) and optical standards. They subsequently revolutionized atomic physics and metrology. The use of frequency combs as an attractive light source for chemistry has been realized

1
2
3 more recently, and their applications to major problems in molecular spectroscopy,
4 chemical kinetics, and sensing are beginning to be borne out. In this Chapter, we
5 highlight emerging techniques using frequency combs that have already enabled new
6 chemical science or that show significant promise in the near future. We give brief
7 context here for some technical aspects of working with comb sources, and also refer the
8 reader to previous comprehensive reviews of the development and evolution of frequency
9 comb technology,³⁻⁶ its particular uses for direct spectroscopy and sensing,⁷⁻⁹ and
10 comparisons between frequency comb systems and other technologies.^{9, 10}

11 The optical frequency comb is a simultaneously broadband and precise light source.
12 It can be thought of as a single laser oscillator emitting thousands of narrow-linewidth
13 continuous-wave (cw) laser lines in parallel, each with well-defined frequency and phase
14 relationships to its neighbors. This unusual light source is the foundation for frequency
15 comb spectroscopy (FCS), a nearly ideal method for kinetics and sensing which (a) is
16 broadband, allowing multiplexed detection of various species and spectral features
17 simultaneously; (b) has excellent frequency resolution, allowing full analysis and
18 identification of the states and species detected; (c) allows high signal-to-noise
19 measurements, to detect trace species or weak features; and (d) has the potential for fast
20 readout, for flexibility of use and to follow chemistry in real time. FCS can meet all of
21 these challenging criteria, often in one experiment. Ongoing technical developments are
22 pushing the capabilities of comb systems to meet these demands, and optimizing their
23 size, simplicity, and ruggedness when deployed in the field.

24 Most frequency combs, though not all, are generated via stabilization of an ultrafast
25 mode-locked laser. In the time domain, a mode-locked laser emits a train of pulses spaced
26 with time period τ or, equivalently, repetition rate f_{rep} (Figure 1). A Fourier transform of
27 this time domain picture to the frequency domain yields a spectrum of discrete optical
28 features, so-called “comb teeth,” evenly spaced by the laser repetition rate. The comb
29 teeth have frequencies ν_m given by

$$\nu_m = m \cdot f_{rep} + f_0 \quad (1)$$

30 where m is an integer and f_0 is a fixed offset frequency common to all teeth. These ν_m
31 correspond to the frequencies of longitudinal modes of the laser oscillator cavity, whose
32 relative phases are constrained by mode-locking to enforce the formation of ultrafast
33 pulses. The f_0 offset, often called the carrier-envelope offset frequency, derives from
34 dispersion within the laser oscillator cavity which causes a pulse-to-pulse phase slip $\Delta\varphi_{CE}$
35 of the oscillating carrier wave with respect to the pulse envelope.

36 Provided that f_{rep} and f_0 are measured and stabilized, these two radiofrequencies
37 constrain the position of every comb tooth and yield a well-determined optical spectrum.
38 It is this feature that allows frequency combs to link RF and optical standards and to
39 serve as a powerful tool for metrology and precision spectroscopy. Determining f_{rep} and f_0
40 is therefore critical to the practical use of frequency combs. Because the intensity of the
41 electric field emitted by a mode locked laser is modulated by f_{rep} , f_{rep} can be accessed
42 simply by measuring the laser output on a photodetector and beating this signal against an
43 RF reference. The measurement of f_0 is more subtle, as the oscillations of the carrier
44 wave are too fast to detect directly. f_0 frequencies are typically measured by self-

referenced $f-2f$ interferometry, wherein a comb is split into two arms, frequency doubled in one arm and broadened in nonlinear fiber in the other to span more than an octave. Beating the $2\nu_n$ comb lines against the nearest ν_m line yields an RF signal at f_0 . The implementation of this interferometry scheme was a historical challenge hindering comb stabilization, until technological breakthroughs in nonlinear fiber development permitted the generation of octave-spanning combs.^{11, 12} f_0 can also be passively cancelled, as is possible for combs derived from difference frequency generation, whose spectra therefore consist solely of integer multiples of f_{rep} .¹³

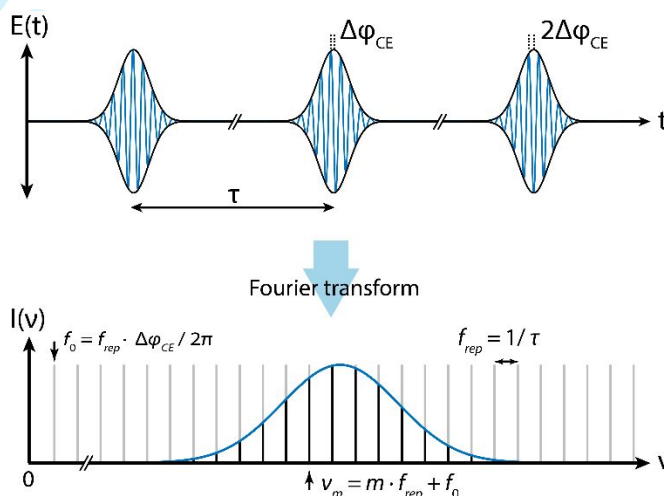


Figure 1. The time domain representation of a mode-locked ultrafast laser pulse train and the corresponding frequency domain representation demonstrating the formation of comb teeth. Reproduced with permission from reference 8. Copyright 2019 Elsevier.

In this Chapter, we emphasize the applications of both stabilized and free-running combs for direct spectroscopy. In direct FCS, comb light is sent through a molecular sample and its spectrum is subsequently recorded, often with resolution of the attenuation of individual comb teeth due to sample absorption. Several laser platforms permit the generation of optical frequency combs relevant to molecular spectroscopy and sensing (Figure 2a), spanning wavelengths from the terahertz (THz) to the extreme ultraviolet (XUV). Direct FCS has now been applied in a variety of sample configurations, including flow cells, high-finesse optical cavities, and open paths in the field (Figure 2b). Various platforms for spectral readout with comb-mode resolution are compatible with these measurements, each with its tradeoffs in acquisition speed, bandwidth, and apparatus complexity (Figure 2c). We now briefly review these relevant experimental components.

While the initial demonstrations of frequency combs based on mode-locked lasers were carried out with solid state Ti:Sapphire systems, fiber-based systems are now the most commonly adopted comb technology. The gain medium of a fiber comb oscillator is a glass fiber doped with rare earth metal cations lasing in the near-infrared (IR), most commonly erbium, ytterbium, or thulium. Fiber lasers have been widely adopted due to a combination of convenient properties: they are robust, relatively inexpensive, and feature

high achievable powers and broad gain bandwidth.¹⁴ Various methods of frequency conversion have been used to extend the native near-IR frequencies of fiber combs to more useful spectral windows. Fiber comb light can be broadened in highly nonlinear fiber to generate a near-IR supercontinuum.¹⁵ Difference frequency generation and optical parametric oscillation in nonlinear crystals have enabled broadband, tunable comb sources spanning visible and mid-IR wavelengths.¹⁶⁻²³ Production of coherent combs in the XUV has been achieved through high harmonic generation carried out in a resonant optical cavity.²⁴

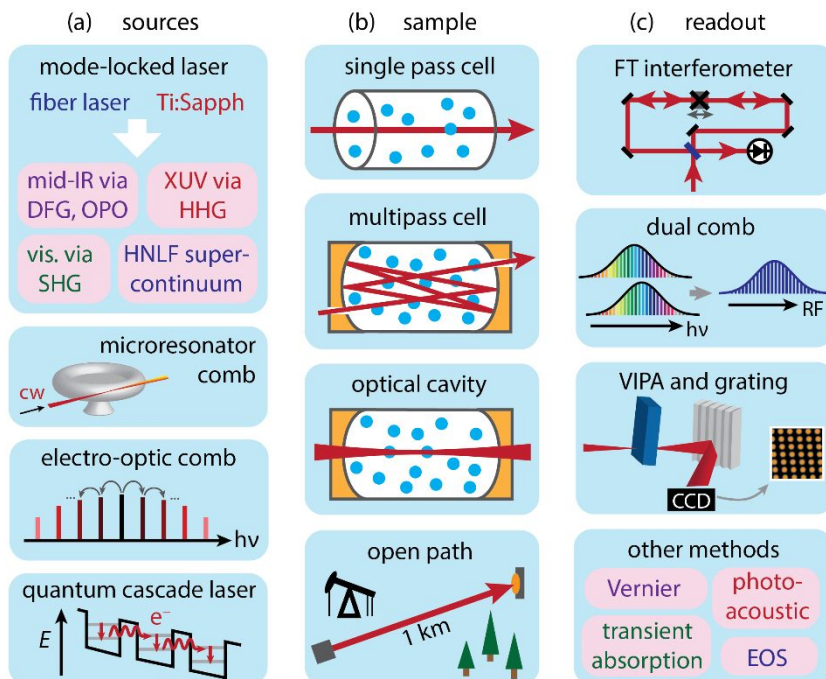


Figure 2. An overview of common (a) frequency comb sources, (b) sample geometries, and (c) spectral readout methods harnessed for molecular spectroscopy, kinetics, and sensing. Abbreviations: DFG, difference frequency generation; OPO, optical parametric oscillator; XUV, extreme ultraviolet; HHG, high harmonic generation; SHG, second harmonic generation; HNLf, highly nonlinear fiber; FT, Fourier transform; VIPA, virtually imaged phased array; EOS, electro-optical sampling.

In recent years, much work has been done to enable novel comb sources that are more compact and frequency agile than mode-locked lasers.^{5,6} Microresonator combs, or microcombs, can be synthesized by coupling a cw laser into a high-quality factor whispering gallery mode resonator or ring resonator where light is confined by total internal reflection. The strong nonlinearities in the resonator material result in four-wave-mixing processes that generate cascaded sidebands on the cw carrier and can form mode-locked soliton pulses.^{25,26} Complete self-referencing²⁷ and dual comb spectroscopy (DCS)²⁸ have recently been demonstrated with microcombs, and there are exciting possibilities for their chip-scale applications. A related development are electro-optic

(EO) combs, wherein cascaded sidebands are placed on a cw carrier using EO modulation.²⁹ In principle, EO combs can be extremely frequency agile, making use of a tunable cw pump laser and a digitally programmable repetition rate. A fully referenced, octave-spanning EO comb has now been demonstrated, though the implementation is technically challenging.³⁰ The development of quantum cascade laser and interband cascade laser frequency combs is also notable, as these semiconductor lasers are the only currently available comb sources that emit directly in the mid-IR and offer electrical rather than optical pumping.^{31, 32} While these systems do not produce ultrafast pulses and have not yet been self-referenced, they show significant promise for free-running mid-IR DCS.^{33, 34}

Combs have been applied to molecular samples in a variety of configurations, some of which are summarized in Figure 2b. Beyond simple single-pass transmission measurements, multipass cells and optical cavities offer significantly improved measurement sensitivity through pathlength enhancement. In particular, the longitudinal mode structure of an optical cavity is a beautiful match for the regularly spaced teeth of a frequency comb, allowing the comb light to be resonantly coupled to the cavity over a broad spectral window.^{7, 35, 36} Open path trajectories are also commonly used for increased sensitivity in comb-based sensing. These configurations will be discussed in the case studies detailed later in this Chapter.

Several methods are widely used to resolve comb spectra following transmission through a sample. Comb-mode resolution is commonly achieved via interferometric readout methods. Fourier transform (FT) interferometry, as used in commercial broadband FT spectrometers, is perhaps the most general method, wherein a scanning delay stage is used to self-interfere comb light to generate an interferogram.³⁷⁻³⁹ The major shortcomings of this technique are the need for mechanical moving parts and correspondingly long acquisition times. DCS is an alternative interferometric method wherein the scanning arm is replaced by a second comb of slightly different repetition rate, $f_{rep} + \Delta f_{rep}$, beat against the first comb on a photodetector to yield an interferogram with repetition rate Δf_{rep} .⁴⁰ DCS allows for rapid, broadband, comb-mode resolved measurements but generally requires two separate combs that are mutually coherent. DCS methods are coming to the fore as comb sources become cheaper and more compact. The use of two EO combs originating from a single cw laser can dramatically reduce DCS apparatus complexity due to high mutual coherence.^{41, 42} Recent work has also pushed to produce dual combs from single laser oscillators,⁴³⁻⁴⁶ and to enable computational coherent averaging techniques to compensate for the spectral instabilities of free running combs.⁴⁷⁻⁵¹

A distinct approach to comb-mode resolution involves spatially dispersing comb light onto a detector array, best demonstrated with virtually imaged phased array (VIPA) etalons^{55, 52} or immersion gratings⁵³ which display very high angular dispersion. A second orthogonal dispersive optical element separates overlapping VIPA mode orders to create a two-dimensional image. The resulting spectrum can be read out with comb-mode resolution^{54, 55} and better than 10 μ s time resolution, making VIPA-based comb spectrometers a powerful tool for chemical kinetics and the detection of transient

1
2
3 molecular species.^{53, 55-58} While the interferometric and dispersive detection methods
4 already mentioned have facilitated the bulk of comb spectroscopies relevant for
5 chemistry, a plethora of other methods have been demonstrated and are worth brief
6 mention here, including electro-optic sampling of THz and mid-IR comb pulses,^{59, 60}
7 Vernier spectroscopy,^{61, 62} broadband photoacoustic spectroscopy,⁶³⁻⁶⁵ cavity-enhanced
8 ultrafast transient absorption,⁶⁶ Ramsey comb spectroscopy,⁶⁷ and comb-based quantum
9 logic spectroscopy.^{68, 69} Some of these developments will be discussed in further detail
10 later on in this Chapter.

11
12 Regardless of detection scheme, if individual comb lines are resolved, the recorded
13 spectrum will be precisely sampled at the native comb tooth spacing f_{rep} . f_{rep} is typically a
14 radiofrequency in the vicinity of a few 100 MHz for mode locked lasers, but can reach
15 10-100 GHz for combs based on microresonator or semiconductor laser architectures.
16 Combs with high repetition rates are useful for DCS, enabling fast acquisition times, and
17 can also be fully mode-resolved with VIPA spectrometers. On the other hand, the more
18 densely sampled spectrum of a lower repetition rate comb is often more appropriate for
19 high-resolution spectroscopy, and comb-mode resolution remains possible with an FT
20 interferometer or DCS. Comb light can also be filtered by locking to an optical cavity
21 with a free spectral range incommensurate with f_{rep} to effectively increase the repetition
22 rate of the transmitted light.⁷⁰ When sampling at f_{rep} is too sparse to capture narrow
23 molecular features, comb spectra acquired with discretely stepped f_{rep} or f_0 can be
24 interleaved. The frequency resolution of a spectrum constructed in this fashion is
25 ultimately limited by the comb tooth linewidth.

26
27 In the following sections we discuss applications of combs to important problems in
28 molecular spectroscopy, chemical kinetics, and sensing, with a focus on recent case
29 studies of particular interest. We conclude with our outlook on the future of comb
30 methods as the technology matures and becomes more widely adopted.

31 32 33 34 **2 Applications**

35 36 37 38 **2.1 Molecular Spectroscopy and Dynamics**

39
40 The benefits afforded by the use of frequency combs as light sources for
41 spectroscopy have enabled enormous breakthroughs in measurements of fundamental
42 molecular structure and dynamics. Combs have now been integrated into a variety of
43 cutting-edge spectroscopic infrastructures yielding drastic improvements in precision,
44 bandwidth, sensitivity, and readout times. Here we place emphasis on work harnessing
45 combs as light sources for direct spectroscopy, though it is important to note that combs
46 have widespread and critical applications in frequency referencing and stabilization of cw
47 experiments. We discuss four frontier case studies in molecular frequency comb
48 spectroscopy, emphasizing state-resolved spectroscopy of large molecules, gas-phase
49 spectroscopy, emphasizing state-resolved spectroscopy of large molecules, gas-phase
50

1
2
3 ultrafast transient absorption, precision studies of molecular ions, and broadband sub-
4 Doppler spectroscopy.
5

6 7 2.1.1 Cavity-enhanced direct comb spectroscopy of large molecules 8

9
10 High-resolution spectroscopy is a powerful tool to reveal the rich internal structure
11 of small molecules in their electronic, vibrational, rotational, and spin degrees of
12 freedom. Achieving a similarly detailed, state-resolved picture of increasingly large
13 molecules is an important frontier, but is subject to stringent experimental requirements.
14 Large molecules have correspondingly large densities of vibrational states, making
15 internal cooling essential to avoid spectral congestion from hot bands. Intramolecular
16 vibrational relaxation (IVR) can cause intrinsic spectral congestion even at relatively low
17 internal energies. A large moment of inertia also leads to very dense rotational structure
18 and demands high spectral resolution.

19
20 Mid-IR cavity-enhanced frequency comb spectroscopy (CE-FCS) applied to
21 cryogenically-cooled molecular samples is a promising combination of methods by which
22 to pursue rovibrational spectroscopy of increasingly large species (Figure 3a).^{71, 72} CE-
23 FCS^{7, 36} is a method of direct FCS wherein the broadband spectrum of comb teeth is
24 resonantly coupled into a series of longitudinal modes of a high-finesse optical cavity
25 surrounding the absorber of interest. Cavity enhancement dramatically improves the
26 sensitivity of absorption measurements via pathlength enhancement while retaining the
27 other advantages of direct FCS.⁷³ Making these absorption measurements in the mid-IR is
28 also critical for studies of large species. In the mid-IR, vibrational fundamental transitions
29 and low-frequency modes are accessible, Doppler broadening is reduced, and low
30 internal energies help avoid congestion from IVR. Cooling the molecules of interest
31 through collisions with an inert buffer gas inside a cryogenic buffer gas cell (CBGC) is a
32 nearly universal means to build significant population in the vibrational ground state and
33 enables the measurement of meaningful structure without obfuscation from hot
34 populations.^{71, 72}
35

36
37 A new record in rovibrational quantum state resolution of large molecules was
38 reported by Changala *et al.* in a CE-FCS study of the C₆₀ fullerene.⁷⁴ C₆₀ is an attractive
39 spectroscopic target due to its rare icosahedral symmetry and importance in
40 astrochemistry. The authors cooled an ensemble of C₆₀ molecules in an intracavity
41 CBGC, quenching vibrational hot bands and thermalizing the sample to a rotational
42 temperature of 150 K. The sample was interrogated with a mid-IR DFG comb near 8.5
43 μm which was spectrally resolved with a scanning arm FT interferometer. A 50 cm^{-1}
44 bandwidth of comb light was simultaneously cavity-coupled and the comb teeth
45 stabilized to 50 kHz linewidths. f_{rep} was stepped to sample the spectrum with a spacing
46 of 3 MHz. Data was acquired for ~ 20 hours, ultimately reaching a noise floor of 0.2 ppm
47 fractional absorption per pass through the cavity, in line with earlier reported sensitivity
48 for this apparatus.⁷²
49
50
51
52
53

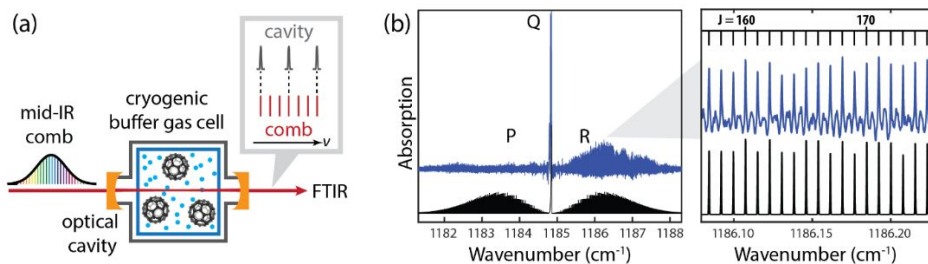


Figure 3. (a) Schematic of a cavity-enhanced frequency comb spectrometer coupled to a cryogenic buffer gas cell containing the absorber of interest. The evenly spaced comb teeth are resonantly coupled into the longitudinal modes of a high-finesse optical cavity. (b) The experimental rovibrational spectrum of cold C_{60} (blue) is plotted against a spherical top simulation fit to the experimental data (black). The cold spectrum exhibits P, Q, and R branches; the R branch in particular (inset) features sharp, well-resolved rovibrational transitions. Figure 3 adapted with permission from reference 74. Copyright 2019 The American Association for the Advancement of Science.

The resulting CE-FCS spectrum reveals a rotationally-resolved vibrational band of C_{60} (Figure 3b). Over 300 R branch transitions were observed and assigned according to their total angular momentum quantum number J . These spectral lines are spaced by ~ 240 MHz and demonstrate 15-30 MHz linewidths governed by a convolution of Doppler and pressure broadening. CE-FCS proved particularly well-suited to resolve the spectrally dense and narrow structure of these features. The R branch transition frequencies were modeled and interpreted with a rovibrational spherical top simulation allowing extraction of extremely precise rovibrational spectroscopic constants of C_{60} for the first time. The combination of CE-FCS and buffer gas cooling is clearly an apt tool for pushing the boundaries of the size and complexity of molecular systems that can be interrogated with complete quantum state resolution, with potential to probe more exotic fullerenes, radicals, and clusters in future work.

2.1.2 Cavity-enhanced ultrafast transient absorption

Broadband cavity-enhancement of frequency combs is powerful for time-resolved spectroscopy in addition to high frequency resolution measurements. Ultrafast spectroscopy gives access to important dynamical information in the time domain, particularly in complex systems where the frequency-domain picture is unresolved or too congested to be interpretable. Ultrafast transient absorption (TA) signals are routinely measured in condensed-phase samples,⁷⁵ but extending this characterization method to dilute gas-phase samples has been an ongoing challenge due to the demanding sensitivity required. While gas-phase ultrafast dynamics are accessible with time-resolved photoelectron-based action spectroscopies, these measurements probe final states and observables that are very different from those of the corresponding solution-phase measurements. Broadband, all-optical TA of dilute gas-phase molecules would provide

1
2
3 direct comparison between ultrafast condensed- and gas-phase measurements made with
4 the same observables.

5 In 2016, Reber *et al.* reported a novel scheme for pump-probe spectroscopy in a low-
6 density molecular beam using cavity-enhanced frequency combs.⁶⁶ The authors harnessed
7 the fact that mode-locked fiber combs supply femtosecond pulses suitable for ultrafast
8 spectroscopy while maintaining discrete teeth that can be resonantly coupled to optical
9 cavities. Reber *et al.* locked pump and probe combs centered at 529 nm to two bow-tie
10 cavities which were spatially overlapped at the molecular beam sample. The resulting
11 enhancement in TA signal is proportional to the product of the pump and probe cavity
12 finesses. The authors observed vibrational beating on the excited state surface of I₂ with a
13 demonstrated ΔOD of 1×10^{-9} Hz^{-1/2}, three orders of magnitude more sensitive than any
14 previous demonstration.⁷⁶ However, this demonstration was made at a single probe
15 frequency of 529 nm with no resolution of the comb spectrum. Expanding this technique
16 to acquire a broadband gas-phase optical spectrum required the development of
17 considerable additional infrastructure, including dispersion-managed broadband optical
18 cavities⁷⁷ and an optical parametric oscillator (OPO) to generate a broadly tunable visible
19 comb.²²

20
21
22 Silfies *et al.*⁷⁸ have now incorporated these developments and reported a fully
23 broadband implementation of cavity-enhanced ultrafast TA, using a 355 nm pump pulse
24 to initiate photochemistry and an OPO probe pulse tunable over the entire visible range
25 from 450-700 nm. The probe comb was coupled into a bow-tie enhancement cavity
26 whose mirrors were designed for minimal group delay dispersion over a wide spectral
27 range. Probe comb pulses with center frequencies spanning the entire visible range can
28 therefore be resonantly coupled with relatively high finesse. The probe cavity maintains
29 the time resolution of comb pulses so that ultrafast TA measurements can be made with a
30 time resolution of ~ 200 fs. As the simultaneous intracavity bandwidth was limited to ~ 10
31 THz, the probe comb's central frequency was scanned in order to construct a broadband
32 spectrum. The authors reported TA of two jet-cooled molecules, 1'-hydroxy-2'-
33 acetophenone and salicylideneaniline, prototypical systems for excited state
34 intramolecular proton transfer. In both systems, Silfies *et al.* measured time constants in
35 line with prior solution-phase measurements but in significant contrast with those
36 measured with time-resolved photoelectron spectroscopies. These results highlight the
37 importance of ultrasensitive, all-optical ultrafast measurements for bridging gas-phase,
38 solution-phase and theoretical work. Additionally, while multidimensional comb
39 spectroscopy has been reported for atomic systems,^{79, 80} it has not yet been demonstrated
40 with molecules or in combination with cavity enhancement. The work of Silfies, Reber,
41 and coworkers could enable the extension of nonlinear methods like two-dimensional IR
42 spectroscopy to dilute gas-phase samples,⁸¹ which currently have no action spectroscopy
43 analogs.
44
45
46
47
48
49
50
51
52
53

2.1.3 Frequency combs for precision spectroscopy of small molecules and ions

Molecular ions are a rich class of species for which precision spectroscopic interrogation has long been a tantalizing target and an experimental challenge. Rotational and vibrational spectroscopy of ions is critical to their identification in astrochemical environments, where rapid, barrierless ion-molecule reactions are believed to drive molecular complexity.^{82, 83} In atomic, molecular, and optical physics, precision spectroscopy of molecular ions enables their utility for studies of ultracold chemistry,⁸⁴ tests of fundamental physics beyond the standard model,⁸⁵ and platforms for quantum information and computing.⁸⁶ Due to their daunting syntheses, extreme reactivity, and low achievable number densities, molecular ions are difficult to prepare and probe in the laboratory.

Action spectroscopies and velocity modulation spectroscopy (VMS) have come to the fore for sensitive state-resolved spectroscopy of molecular ions. The integration of optical frequency combs for referencing and readout have dramatically enhanced the precision of these measurements. In most ion action spectroscopies, ions are excited with scanned cw laser radiation and the effects of resonant absorption are monitored via resulting changes to the mass spectrum. Absolute referencing of the cw laser frequency to a comb has enabled measurements with sub-MHz resolution,⁸⁷ including studies of benchmark astrochemical systems like the H_3^+ cation,⁸⁸ and extremely challenging targets like the fluxional CH_5^+ cation.⁸⁹ VMS is a complementary technique wherein the electric field of the ion discharge source is modulated, causing an oscillating Doppler shift of ion absorption features that can be detected with a lock-in amplifier. VMS techniques are almost always used with absolute frequency comb referencing of the cw laser light to achieve spectral uncertainties on the few-MHz level.⁹⁰ Cavity-enhanced VMS has also been successfully implemented with a broadband comb as the direct light source.^{91, 92}

A recent development in comb-based ion spectroscopy is the work of Chou *et al.* to interrogate the THz rotational transitions of a single molecular ion using frequency comb Raman spectroscopy and quantum logic techniques.⁶⁹ A single $^{40}\text{CaH}^+$ ion was co-trapped in an ion trap with a laser cooled $^{40}\text{Ca}^+$ ion. The quantum state of $^{40}\text{CaH}^+$ was first prepared using quantum logic spectroscopy.⁸⁶ The authors then coherently drove stimulated THz Raman rotational transitions in $^{40}\text{CaH}^+$ using two arms of a stabilized Ti:Sapph frequency comb. The probability that the Raman transition occurred was measured using quantum logic spectroscopy as the comb tooth frequencies were scanned. Rotational transition frequencies were reported with uncertainties at the kHz level, limited by the coherence of the stabilized comb, which could be improved to the Hz level or better in future work. This technique can also be adapted to Raman measurements of IR, rather than THz, transitions by using increasingly broadband combs. Since the Raman comb laser is detuned from resonance, it is not specific to this molecular system and can in principle be harnessed for studies of more complex polyatomic ions of chemical interest.

2.1.4 Broadband sub-Doppler spectroscopy with frequency combs

Frequency combs are continually being integrated in novel experimental configurations for broadband precision spectroscopy. Doppler broadening due to the thermal distribution of velocities in an ensemble of absorbers is often the limiting factor in the spectral linewidths of gas-phase species, presenting an intrinsic constraint for high-resolution measurements. Sub-Doppler spectroscopies make use of intense illumination with a spectrally narrow pump laser to transfer a significant fraction of a specific velocity class of molecules from one state to another. The resulting spectral signatures are governed by homogeneous broadening processes rather than Doppler broadening. Observation of these sub-Doppler signatures can be critical not only for precision measurements, but for disentangling congested spectra where state splittings fall within the Doppler linewidth. However, sub-Doppler measurements remain typically limited by the accuracies and tuning ranges of the lasers involved. Foltynowicz *et al.* recently reported a sub-Doppler double resonance spectroscopy (DRS) scheme using a frequency comb as a broadband probe.^{93, 94} The authors applied this apparatus to study the vibrational overtones of the ν_3 mode of methane (CH_4). Spectral data on highly vibrationally-excited states of CH_4 are important for benchmarking theoretical predictions of high-temperature spectra, with intriguing applications for spectroscopy of exoplanet atmospheres.⁹⁵ While comb-referenced DRS methods have been used previously to great effect,⁹⁶⁻⁹⁸ and sub-Doppler comb spectroscopy has been reported for atomic systems,⁹⁹ this work represents the first sub-Doppler work using direct FCS on any molecular system.

DRS is a common implementation of sub-Doppler spectroscopy. A narrow linewidth pump laser saturates a specific rovibrational transition, and a probe laser measures depletion features in transitions that share a common lower state with the pumped transition (V type transitions) or the appearance of new excited state absorption features (ladder transitions), as shown in Figure 4a and 4b for both cw and comb probes. Foltynowicz *et al.* used a Lamb dip lock to stabilize a cw pump laser to a series of nine distinct rovibrational lines of CH_4 near 3.3 μm . The comb probe near 1.67 μm allowed for simultaneous detection of more than 10,000 spectral elements over a 200 cm^{-1} bandwidth, detected via scanning arm FT interferometer with comb mode resolution and a noise equivalent absorption coefficient of $7.2 \times 10^{-6} \text{ cm}^{-1}$ after 3.2 hours of averaging. The probe comb f_{rep} was scanned to sample the spectrum with 2 MHz steps.

The combination of wide spectral coverage and high frequency accuracy of Foltynowicz and coworkers' probe comb enabled the detection of 18 sub-Doppler V-type rovibrational transitions between the vibrational ground state and the $2\nu_3$ band (Figure 4c) and 36 novel $3\nu_3 \leftarrow \nu_3$ ladder-type transitions. The authors reported orders-of-magnitude better frequency precision than prior spectroscopic studies of the $3\nu_3$ manifold of CH_4 .¹⁰⁰ The ultimate frequency accuracy of these measurements remains limited to ~ 1 MHz by the stabilization of the cw pump laser. Stabilizing the cw pump laser via frequency comb referencing could ultimately improve the resolution to the kHz level.^{97, 98} The addition of an enhancement cavity for the broadband comb probe could improve sensitivity and

enable the extension of these measurements to more challenging spectroscopic targets that cannot be prepared in high concentration.

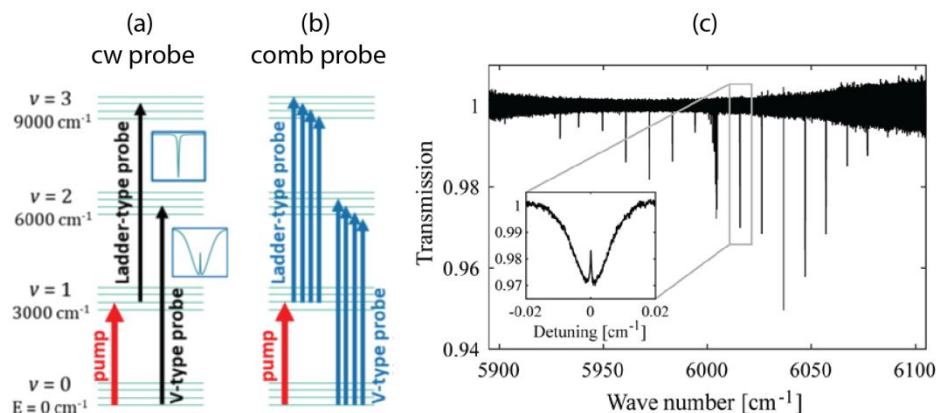


Figure 4. *V*-type and ladder-type double resonance transitions studied in the v_3 overtone transitions of methane with a (a) cw or (b) frequency comb probe. (c) Comb probe spectrum of methane near 6000 cm^{-1} acquired with the pump laser on resonance with the v_3 fundamental $R(0)$ transition, showing a subsequent *V*-type probe transition in the $2v_3$ overtone $R(0)$ transition. Figure 4 adapted with permission from reference 93. Copyright Foltynowicz et al., some rights reserved; exclusive licensee American Physical Society.

Distributed under a Creative Commons Attribution License 4.0 (CC BY)

<https://creativecommons.org/licenses/by/4.0/>

2.2 Chemical Reaction Kinetics

A natural application of FCS is the measurement of spectra of reacting mixtures as a function of time, akin to *in situ operando* spectroscopy used in the field of catalysis.¹⁰¹ Understanding reaction kinetics is fundamental to all areas of chemistry, ranging from fuel combustion to protein folding dynamics.¹⁰² The quantitative determination of reaction rate coefficients and product branching ratios yields insight into reaction mechanisms, which can, in turn, enable prediction and control of chemical transformations.

One strong advantage of FCS is the naturally multiplexed information that can be gathered in a kinetics experiment. The identifying features of reactants, intermediates, and products can potentially be monitored within a single spectral window spanning upwards of 100 cm^{-1} depending on the methodology employed. Reaction rate coefficients can subsequently be extracted from the temporal evolution of these spectra. The measurement of coupled kinetic information – for instance the rate of decay of a reactant being equal to the rate of appearance of an intermediate – may elucidate a complex reaction potential energy surface. In addition, if all product pathways from a reaction are spectroscopically identified and their rate coefficients for production are measured, the

1
2
3 product branching ratios can be determined. A second advantage of FCS methods is the
4 ability to measure several spectral features of a single species at once. More precise
5 reaction rate coefficients can be derived by monitoring multiple transitions or even an
6 entire spectrum associated with the same molecule as a function of time.

7
8 The sheer volume of data and information contained in a single FCS kinetics
9 experiment can appear daunting, but ultimately presents spectacular possibilities to
10 elucidate complex chemical reaction mechanisms. Unless all molecules involved in the
11 reaction have well-characterized spectra, then what is nominally a kinetics experiment
12 will always require potentially high-level spectral analysis alongside kinetic data
13 analysis. In addition, peaks may be observed that are not assigned to molecules taking
14 part in the reaction. This abundance of spectral and kinetic data presents an exciting
15 opportunity to fully understand chemical reactions. For example, the reaction of $\text{OD} +$
16 $\text{CO} \rightarrow \text{D} + \text{CO}_2$ is fundamental to both atmospheric and combustion chemistry, and was
17 one of the first chemical reaction kinetics studies reported using FCS.⁵⁶ Bjork *et al.* used
18 CE-FCS to explicitly capture the role of the DOCO reaction intermediate for the first
19 time. The authors measured vibrational spectra of the *cis*- and *trans*-DOCO isomers and
20 determined their independent reaction rate coefficients for growth and decay.¹⁰³⁻¹⁰⁵ After
21 simulating and accounting for the IR signatures of the reactants, intermediates, and
22 products of the $\text{OD} + \text{CO} \rightarrow \text{D} + \text{CO}_2$ reaction, additional spectral features were observed
23 in the broadband comb spectra that did not directly involve these molecules. These peaks
24 were ultimately accounted for by water and its isotopes, all of which have known IR
25 spectra. The presence of a trace amount of water in both the reaction cell and the
26 spectrum did not significantly impact the kinetic analysis.

27
28 Chemical kinetics can, of course, also be studied using more conventional direct
29 absorption methods, including step-scan Fourier transform IR (FTIR) spectrometers,
30 scanning narrowband lasers, or incoherent broadband light sources in combination with
31 dispersive spectrometers. These methods have drawbacks, including limitations in
32 achievable spectral resolution or lengthy laboratory data collection times, which can
33 expose the study to long-timescale fluctuations. Step-scan FTIR can also achieve spectral
34 multiplexing, but can take an order of magnitude more laboratory time to achieve the
35 same time and spectral resolution as FCS methods.^{106, 107} Additionally, unlike a comb, the
36 incoherent FTIR light source cannot be efficiently coupled into an optical enhancement
37 cavity, potentially limiting the sensitivity of the measurement.

38
39 Given the multiplexing and sensitivity advantages of FCS, along with spectral
40 readout on the microsecond timescale, combs are being integrated into a wide variety of
41 chemical kinetics studies. We now discuss recent case studies in the application of combs
42 to reaction kinetics, targeting examples in both gas-phase and solution-phase
43 environments.
44

2.2.1 Gas-phase Criegee intermediate reaction kinetics

Several research groups are actively applying FCS to gas-phase chemical reaction kinetics, harnessing both dual-comb and spatially dispersive methods to study reacting systems in room temperature flow cells,^{56, 58, 108-113} and high temperature flames, discharges, and shock tubes.¹¹⁴⁻¹²² The application of these methods to problems in atmospheric chemistry is particularly compelling. One recent room temperature FCS flow cell study by Luo *et al.* concerns the formation and subsequent reaction of the simplest Criegee intermediate, CH₂OO.^{110, 111} Criegee intermediates are a class of zwitterions formed from the ozonolysis of alkenes, and their subsequent reactions have impacts on processes ranging from aerosol formation to the oxidative chemistry of the troposphere.¹²³ Criegee chemistry has been an active area of research in atmospheric physical chemistry since 2012 when the laboratory synthetic route to forming CH₂OO was established.¹²⁴ Since then, IR and ultraviolet (UV) absorption spectroscopies and time-of-flight mass spectrometry have been used to study the reactions of Criegee intermediates with other atmospherically relevant molecules.¹²⁵

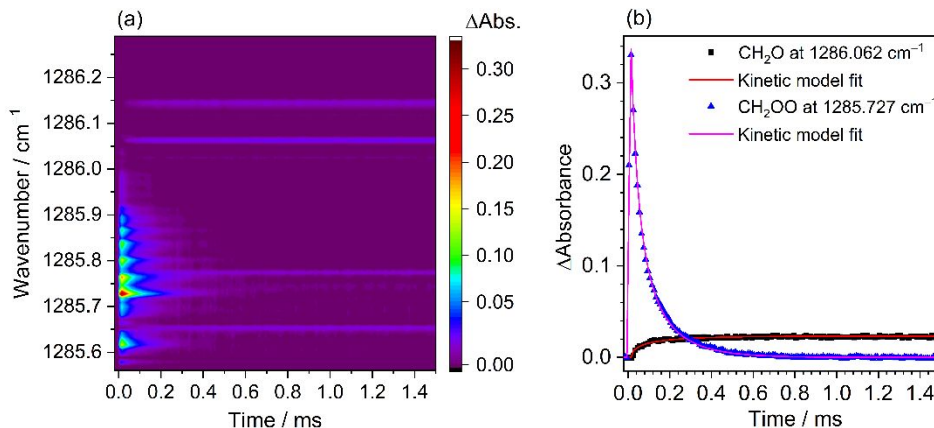


Figure 5. (a) Time-resolved DCS of Criegee chemistry near 1286 cm^{-1} . The spectra were recorded after the 248 nm irradiation of a flowing mixture of CH₂I₂/O₂ over 8000 excimer laser shots. The spectral sampling spacing was 279 MHz ($9.3 \times 10^{-3}\text{ cm}^{-1}$), and the temporal resolution was 10 μs . (b) Temporal profiles of a CH₂O line at 1286.062 cm^{-1} and a CH₂OO absorption peak at 1285.727 cm^{-1} . [CH₂OO]₀ was estimated to be $5.6 \times 10^{13}\text{ molecule cm}^{-3}$ by kinetic model fitting of the time traces. Adapted with permission from reference 111. Copyright 2020 The Optical Society.

The laboratory synthetic route for the formation of CH₂OO proceeds via the UV photolysis of diiodomethane (CH₂I₂) in the presence of O₂. The resulting CH₂I radical readily reacts with an excess of O₂ to form CH₂OO. The subsequent reaction of CH₂OO with other atmospherically relevant molecules is typically carried out under pseudo first-order conditions. The decay of [CH₂OO] is measured as a function of time relative to the initiating photolysis laser pulse, taken to occur at $t = 0$. Luo *et al.* monitored the self-reaction of CH₂OO to form formaldehyde (CH₂O) via vibrational signatures using EO

1
2
3 DCS in the long-wave mid-IR near 1285 cm^{-1} , shown as a function of time in Figure
4 5a.^{110, 111} At short time delays following photolysis, the observed spectral peaks
5 corresponded to the ν_4 fundamental vibrational band of CH_2OO . At longer times, part of
6 the CH_2O ν_6 fundamental vibrational band grew in. Whilst a fit to the whole spectrum
7 could be used to measure the decay of $[\text{CH}_2\text{OO}]$ and growth of $[\text{CH}_2\text{O}]$ shown in Figure
8 5b, a single peak was chosen for each species. The coupled decay and growth traces of
9 $[\text{CH}_2\text{OO}]$ and $[\text{CH}_2\text{O}]$ were consistent with previous kinetic models of the CH_2OO self-
10 reaction.¹²⁶

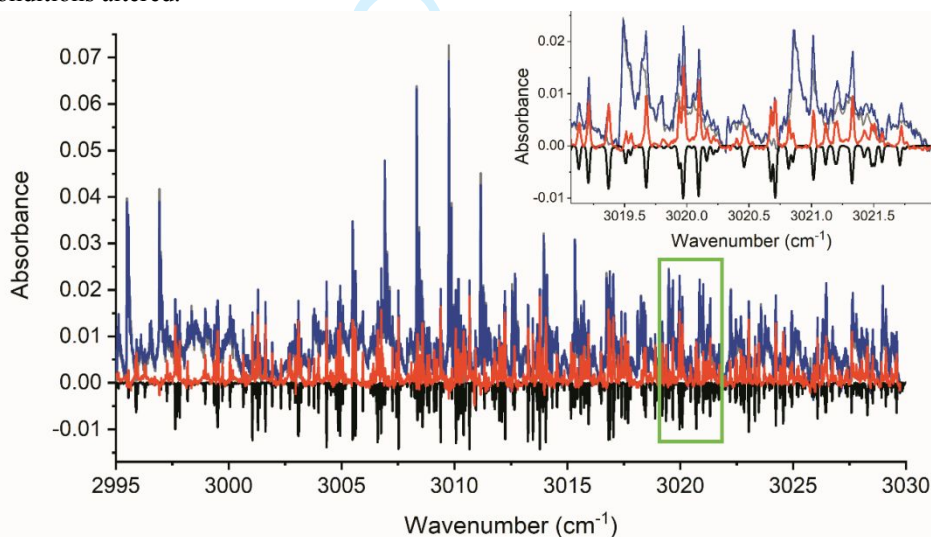
11
12 It is informative to compare the capabilities of the EO DCS system of Luo *et al.*
13 against a chirped-pulse QCL system previously used to measure the ν_4 absorption
14 spectrum of CH_2OO .¹²⁷ Using the QCL method, a similar spectral window of 1.5 cm^{-1}
15 was gathered with a time resolution of $240\text{ }\mu\text{s}$. The QCL experiments demonstrated a
16 baseline absorbance noise level of 2.5×10^{-4} over 90 laser shots. In the DCS experiments
17 described above, the baseline absorbance noise level was 7.1×10^{-4} when averaging a $6\text{ }\mu\text{s}$
18 integration time for 16,000 laser shots. Although the noise floor is somewhat higher for
19 the DCS experiment, the time resolution is considerably better for measuring fast
20 kinetics. In addition, the time resolution and spectral bandwidth in a DCS experiment are
21 inherently coupled by the Nyquist criterion for a given data point spacing.¹²⁰ The DCS
22 experiment is therefore limited to a narrow wavelength range simply for the purposes of
23 achieving the best time resolution ($6\text{ }\mu\text{s}$). The spectral range can be broadened with a
24 corresponding compromise in time resolution. The central wavelength of the
25 measurement can also be tuned over the wider $1215\text{--}1287\text{ cm}^{-1}$ range available to the
26 laser system. The DCS apparatus is therefore time and frequency agile, depending on the
27 needs of a given experiment. A more traditional step-scan FTIR instrument can also be
28 used for CH_2OO spectroscopy and kinetics, as demonstrated by Su *et al.*¹²⁸ and later by
29 Huang *et al.*¹²⁹ In these studies, a broader spectral bandwidth (e.g. $750\text{--}1500\text{ cm}^{-1}$) was
30 achieved using an incoherent light source while maintaining nanosecond to microsecond
31 time resolution. However, the instrument resolution was limited to $0.25\text{--}1\text{ cm}^{-1}$. Not
32 enough information is given on noise levels to compare these experiments to EO DCS.

33
34 Long-wave mid-IR FCS experiments like the study detailed above currently rely on
35 DCS rather than spatially dispersive methods. High-resolution dispersive optical elements
36 and cameras operating in the long-wave mid-IR require custom fabrication and can be
37 prohibitively expensive, although long-wave mid-IR FCS using dispersive detection was
38 recently showcased using an immersion grating.⁵³ In the short-wave mid-IR near 3000 cm^{-1} ,
39 however, dispersive comb techniques can be harnessed to study Criegee chemistry
40 via C–H stretching signatures of the reactants, intermediates, and products.

41
42 The Lehman Research Group at the University of Leeds recently used the photolysis
43 of CH_2I_2 and resulting laser-induced signals to commission a new dispersive frequency
44 comb spectrometer. CH_2I_2 is a useful target when constructing a new instrument because
45 of its large photolysis cross section ($>1\times 10^{-18}\text{ cm}^2\text{ molecule}^{-1}$) in an easily accessible
46 region of the UV ($248\text{--}355\text{ nm}$). CH_2I and CH_2 are subsequently formed in single photon
47 and multiphoton processes, respectively. This study used a 250 MHz repetition rate mid-
48 IR comb spanning $2700\text{--}3300\text{ cm}^{-1}$ and a spatially dispersive FCS spectrometer with ~ 35
49
50
51
52
53

1
2
3 cm^{-1} simultaneous coverage.⁵⁸ An IR spectrum was acquired at a 400 μs time delay
4 following photolysis (Figure 6). A spectral signature can be seen in the difference
5 spectrum (red) of the photolysis laser on (blue) and laser off (grey) datasets. The
6 observed peaks in the difference spectrum were almost entirely accounted for by $\sim 7 \times 10^{13}$
7 molecule cm^{-3} ethylene (C_2H_4), which was modeled using its known IR absorption
8 spectrum from the HITRAN database (black)¹³⁰ convolved with the expected Doppler
9 broadening and instrument lineshape function.

11 The observation of C_2H_4 was unexpected, although its presence yields insight into
12 the experimental conditions and highlights the benefit of collecting broadband, high-
13 resolution kinetics spectra potentially containing unknown spectral signatures. Under
14 room temperature flow cell conditions, it is relatively easy to produce unintended
15 reaction products if the gas refresh rate is slow compared to the photolysis laser repetition
16 rate, as was the case here. Ethylene was likely formed from sequential photolysis laser
17 pulses interacting with the gas sample, creating both CH_2 and CH_2I which then react to
18 form C_2H_4 . By using a broadband, high-resolution detection method with sufficient
19 sensitivity, in addition to finding new reaction products or intermediates, any unintended
20 reaction products or contaminant species can be identified and the experimental
21 conditions altered.

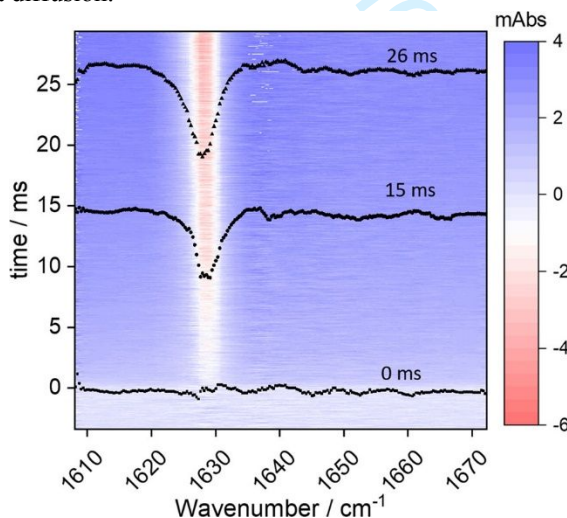


23
24
25
26
27
28
29
30
31
32
33
34
35
36
37
38
39
40 **Figure 6.** IR absorption spectra following the photolysis of CH_2I_2 (5×10^{16} molecule cm^{-3} ,
41 20 mbar total pressure) at 266 nm. Spectra are shown for photolysis laser on (blue) and
42 laser off (grey). The laser off absorption trace is dominated by CH_2I_2 features. The
43 difference spectrum (red, photolysis laser on – laser off) is well-modeled by the C_2H_4 IR
44 spectrum (HITRAN, black, inverted). Data were taken at 10 Hz (photolysis laser
45 repetition rate) with 50 μs integration time at $\Delta t(\text{camera} - \text{photolysis laser}) = 400 \mu\text{s}$,
46 averaging for 2000 images.

2.2.2 Liquid-phase monolayer desorption kinetics

Although the full advantages of simultaneously broadband and high-resolution frequency comb light sources are perhaps most ideally matched to gas-phase studies, where linewidths are typically limited by Doppler broadening, there have been a number of successful liquid-phase studies employing DCS methods.^{106, 107, 131-138} Since the achievable spectral resolution in condensed phase spectroscopy is usually governed by inhomogeneous solvent interactions rather than instrument limitations, larger comb repetition rates are sufficient. Major applications of DCS to liquid-phase kinetics range from simple organic reactions¹³³ to irreversible protein reactions.^{107, 134}

DCS has been employed in attenuated total reflectance (ATR) spectrometers, used for studying liquid-phase reactions and monolayer deposition processes.^{106, 133} Lins *et al.* recently studied the spectroelectrochemistry of the desorption of a monolayer of a pyridine derivative.¹⁰⁶ A commercial QCL-based DCS instrument was coupled into an ATR-surface-enhanced IR absorption spectroscopy (SEIRAS) accessory, which was adapted for a laser light source instead of the usual broadband incoherent light source. The authors prepared a gold nanoparticle film on top of an indium tin oxide layered silicon internal reflection element, and adsorbed a monolayer of 4-dimethylaminopyridine (DMAP). Whilst this pyridine derivative was chosen as a proof-of-concept target, its use in organic films and molecular devices is well documented.^{139, 140} DMAP was desorbed from the gold surface by applying a potential jump, and the 1610–1670 cm^{-1} IR spectrum was collected as a function of time (Figure 7). The transient IR signal observed near 1628 cm^{-1} was assigned to several ring vibrational modes of DMAP. The decrease in absorbance signal showed evidence for the desorption process, allowing for the measurement of time constants for the desorption of DMAP from gold and its subsequent diffusion.



1
2
3 **Figure 7.** Time-resolved evolution of the ATR-SEIRAS absorbance change upon DMAP
4 desorption from a gold surface, following a potential jump from +0.30 to -0.90 V,
5 acquired using a mid-IR dual-comb spectrometer. Spectral processing conditions were
6 128 coadditions with 20 μs time binning. Spectral resolution was 3.3 cm^{-1} . Reproduced
7 with permission from reference 106. Copyright 2020 American Chemical Society.
8
9

10 The study by Lins *et al.* demonstrates the potential for ATR DCS to replace step-
11 scan FTIR ATR-SEIRAS. The detection limit of the DCS experiment was approximately
12 0.08 mAbs, or 0.7% of the monolayer, using a time resolution of 800 μs and spectral
13 resolution of 3.3 cm^{-1} . A step-scan FTIR spectrometer can achieve similar sensitivity and
14 time resolution with a lower 8 cm^{-1} spectral resolution. The most striking point of
15 comparison, however, is the laboratory time necessary to achieve these levels of
16 sensitivity with comparable temporal resolution. Conventional step-scan FTIR requires
17 the equivalent of 2 days of laboratory time, while the DCS experiment takes 32 minutes.
18 The implementation of DCS by Lins *et al.* used a QCL operating over a much smaller
19 spectral window compared to the broadband incoherent light source used in conventional
20 methods. However, DCS clearly has an enormous advantage in laboratory time if the
21 target wavelength for a given experiment falls within the QCL operating wavelength
22 range.
23
24

25 26 **2.3 Molecular Sensing** 27

28 We finally turn our attention to implementations of FCS for analytical sensing. Here
29 we define sensing as the identification and quantification of steady-state concentrations
30 of molecules present in a mixture using known spectral signatures. Molecular sensing is a
31 robust application of FCS with huge potential across many different fields^{116, 141-153} due to
32 the unique attributes of comb instrumentation already emphasized throughout this
33 Chapter. The analytical chemistry applications of FCS include characterizing emissions
34 in storage facilities,¹⁴⁴ accurately measuring temperatures and quality factors of
35 combustion environments,^{116, 152} and human breath analysis for medical diagnostics.^{35, 154,}
36 ¹⁵⁵ The success and widespread adoption of combs for sensing are highly dependent on
37 rapidly developing technological advances, as discussed by Ycas *et al.*¹⁴³ and references
38 therein. Sensing applications also show significant promise in introducing combs to a
39 broader scientific audience and the general public.
40
41

42 A distinct advantage of FCS – and laser absorption spectroscopy techniques more
43 generally – for sensing is the highly directional nature of their detection and the potential
44 for long distance propagation.¹⁵⁶ This enables long-path measurements, including
45 atmospheric monitoring of pollutants and tracking natural gas leaks across a large open
46 field.^{148, 149, 153} FCS is also calibration-free and allows for simultaneous monitoring of
47 numerous molecules. As we have discussed throughout this Chapter, FCS can be used to
48 probe various environments under a wide range of experimental conditions.
49
50

1
2
3 FCS, particularly DCS methodology, has made significant strides in becoming
4 compact, user-friendly, and field-deployable with low power consumption.¹⁴³ These are
5 attractive qualities to position DCS as a viable alternative to other passive sensing
6 techniques. In addition, technological advances in comb and fiber technology enable
7 researchers to access the chemically important mid-IR in field-deployable
8 instrumentation while still covering a broadband spectral range. These instruments are
9 therefore no longer limited to probing weak vibrational overtones in the near-IR nor are
10 they limited to laboratory environments. To give a specific example, Ycas *et al.* measured
11 concentrations of volatile organic compounds (VOCs) including ethane and propane in
12 open-path field experiments using a DCS instrument spanning 2750–3150 cm⁻¹ with
13 0.0067 cm⁻¹ resolution. After signal processing, this new instrument achieved a
14 sensitivity dependent on the path length and integration time of $120 \text{ ppb} \cdot \text{m} \cdot \sqrt{\text{minutes}}$
15 .¹⁴³ Continuous measurements of up to 30 hours of data were taken for a 120 m open
16 path, highlighting the stability of this instrumentation.
17

18
19 Depending on the molecular targets, it might seem challenging to outpace cost-
20 effective and user-friendly techniques such as chemometric and eNose sensors, or the
21 highly sensitive established techniques of chromatography and mass spectrometry.¹⁵⁷ The
22 UK Department for Environment Food & Rural Affairs (Defra) serves as a useful
23 benchmark. Defra uses Perkin Elmer Ozone Precursor gas chromatography-flame
24 ionization detector systems stationed at multiple locations as part of their automated
25 hydrocarbon monitoring network. Hourly measurements of concentrations of close to 30
26 different VOCs are taken by sampling the air at the instrumentation site.¹⁵⁸ This
27 chromatography instrument has limits of detection in the low parts-per-billion (<0.1 ppb)
28 for various VOC pollutants, but needs to be calibrated using a gas mixture standard. The
29 mid-IR field-deployable DCS instrument of Ycas *et al.* can reach the ppb sensitivity
30 necessary to monitor atmospheric VOCs, similar to the more conventional
31 chromatography methods but without the need for calibration. Moreover, the DCS
32 instrumentation can take continuous, open-path measurements in a directional manner,
33 yielding VOC concentration and identification profiles as a function of location and time.
34 This capability may prove of extreme utility in industrial settings as well as for
35 environmental monitoring and atmospheric modeling of tropospheric chemistry.^{159, 160}
36
37
38

39 40 41 42 43 44 45 46 47 48 49 50 51 52 53 54 55 56

3 Conclusions and Outlook

In this Chapter, we have surveyed the current state of frequency comb spectroscopy and its myriad applications in observing and understanding chemical phenomena. It is now demonstrated that combs can replace incoherent and narrowband light sources in most direct absorption spectroscopy experiments, improving the precision and sensitivity of these measurements as well as the laboratory timescales for data collection.

Frequency combs have enabled great strides forward in fundamental laboratory spectroscopy and dynamics. We reviewed several recent high-impact studies where the capabilities of FCS infrastructure have elucidated the structure of challenging

1 spectroscopic targets that proved inaccessible with other techniques. Combs are of
2 particular utility for precision spectroscopy, with frequency resolution unconstrained by
3 instrument lineshapes. In combination with cryogenic buffer gas cooling techniques, FCS
4 has enabled state-resolved measurements of unprecedentedly large fullerene molecules.
5 The size limit for quantum state resolution has certainly not yet been reached; moving to
6 lower internal temperatures with improved cooling and longer mid-IR wavelengths
7 should permit the study of even larger systems. The applications of direct comb methods
8 for ion spectroscopy and sub-Doppler measurements are similarly not far past the proof-
9 of-concept stage, and can be extended to considerably more complex molecular species
10 of broad chemical interest. The realization of frequency combs as femtosecond light
11 sources that can be resonantly coupled to optical cavities has ushered in a new era of all-
12 optical ultrasensitive, ultrafast measurements in dilute gas-phase samples.

13 Combs are also now widely applied to probe chemical reaction kinetics on the
14 microsecond to millisecond timescale in both gas- and liquid-phase environments. We
15 highlighted particular applications in atmospheric chemistry and monolayer desorption
16 experiments to showcase their utility across various fields of chemistry. Kinetics
17 measurements under extreme conditions can inform our understanding of chemistry in
18 environments ranging from combustion engines to regions of the interstellar medium.
19 Low temperature kinetics studies can provide detailed information on reaction potential
20 energy surfaces, such as the presence of submerged or low-lying barriers to reaction. Low
21 temperature experiments are currently under construction in at least two different
22 research groups at the University of Leeds and the Université de Rennes, combining a
23 cold molecular flow produced using a Laval expansion with FCS detection.¹⁶¹ The future
24 of comb-based chemical reaction kinetics could see expansion of chemical applications
25 or the use of alternative spectroscopic probes including THz radiation.¹¹³

26 Outside of the physical chemistry laboratory, molecular sensing will likely become a
27 highly successful application of FCS, particularly with the development of lower cost,
28 miniaturized systems. In this Chapter, we emphasized the recent use of FCS for open-
29 path environmental monitoring measurements. Novel sensing applications may include
30 the integration of FCS as a passive in-line spectroscopic probe of industrial scale flow
31 chemistry¹⁶² or as a hospital bedside breath gas analyzer aimed at identifying
32 biosignatures for disease diagnosis.¹⁶³ Further development of FCS technologies
33 surrounding sensing applications are likely to result in broader scientific and general
34 public involvement, creating a feedback loop of investment and technological expansion.

35 Optical frequency combs have proved to be powerful spectroscopic tools due to their
36 precision, bandwidth, potential for high sensitivity measurements, and rapid experimental
37 readout times. The ability to collect multiplexed information in a single experiment is a
38 significant advantage in many of the applications discussed herein. At present, save for a
39 few high-impact spectroscopic and kinetics studies, most of the recent chemical
40 applications of FCS are proof-of-concept or benchmarking experiments. As comb
41 technology matures and reaches more laboratories, we expect that an accompanying
42 expansion of chemical applications will become evident. We anticipate that the coming
43 years will yield new comb-based demonstrations of precision spectroscopy for tests of

1
2
3 fundamental physics, resolved sub-Doppler structure in unprecedentedly complex
4 molecular systems, sensitive probes of cold chemistry and kinetics, new limits on the
5 detection of ultrafast reaction dynamics, and integration with microscopy for applications
6 in biology and nanoscience.
7

4 References

1. Hall, J. L., Nobel Lecture: Defining and Measuring Optical Frequencies. *Rev Mod Phys* **2006**, *78*, 1279-1295.
2. Hänsch, T. W., Nobel Lecture: Passion for Precision. *Rev Mod Phys* **2006**, *78*, 1297-1309.
3. Cundiff, S. T.; Ye, J., Femtosecond Optical Frequency Combs. *Rev Mod Phys* **2003**, *75*, 325-342.
4. Diddams, S. A., The Evolving Optical Frequency Comb. *J Opt Soc Am B* **2010**, *27*, B51-B62.
5. Fortier, T.; Baumann, E., 20 Years of Developments in Optical Frequency Comb Technology and Applications. *Commun Phys* **2019**, *2*, 16.
6. Diddams, S. A.; Vahala, K.; Udem, T., Optical Frequency Combs: Coherently Uniting the Electromagnetic Spectrum. *Science* **2020**, *369*, eaay3676.
7. Adler, F.; Thorpe, M. J.; Cossel, K. C.; Ye, J., Cavity-Enhanced Direct Frequency Comb Spectroscopy: Technology and Applications. *Annu Rev Anal Chem* **2010**, *3*, 175-205.
8. Weichman, M. L.; Changala, P. B.; Ye, J.; Chen, Z.; Yan, M.; Picqué, N., Broadband Molecular Spectroscopy with Optical Frequency Combs. *J Mol Spectrosc* **2019**, *355*, 66-78.
9. Picqué, N.; Hänsch, T. W., Frequency Comb Spectroscopy. *Nat Photonics* **2019**, *13*, 146-157.
10. Cossel, K. C.; Waxman, E. M.; Finneran, I. A.; Blake, G. A.; Ye, J.; Newbury, N. R., Gas-Phase Broadband Spectroscopy Using Active Sources: Progress, Status, and Applications. *J Opt Soc Am B* **2017**, *34*, 104-129.
11. Jones, D. J.; Diddams, S. A.; Ranka, J. K.; Stentz, A.; Windeler, R. S.; Hall, J. L.; Cundiff, S. T., Carrier-Envelope Phase Control of Femtosecond Mode-Locked Lasers and Direct Optical Frequency Synthesis. *Science* **2000**, *288*, 635-639.
12. Reichert, J.; Niering, M.; Holzwarth, R.; Weitz, M.; Udem, T.; Hänsch, T. W., Phase Coherent Vacuum-Ultraviolet to Radio Frequency Comparison with a Mode-Locked Laser. *Phys Rev Lett* **2000**, *84*, 3232-3235.
13. Schliesser, A.; Picqué, N.; Hänsch, T. W., Mid-Infrared Frequency Combs. *Nat Photonics* **2012**, *6*, 440-449.
14. Kim, J.; Song, Y. J., Ultralow-Noise Mode-Locked Fiber Lasers and Frequency Combs: Principles, Status, and Applications. *Adv Opt Photonics* **2016**, *8*, 465-540.
15. Sinclair, L. C.; Deschenes, J.-D.; Sonderhouse, L.; Swann, W. C.; Khader, I. H.; Baumann, E.; Newbury, N. R.; Coddington, I., Invited Article: A Compact Optically Coherent Fiber Frequency Comb. *Rev Sci Instrum* **2015**, *86*, 081301.
16. Adler, F.; Cossel, K. C.; Thorpe, M. J.; Hartl, I.; Fermann, M. E.; Ye, J., Phase-Stabilized, 1.5 W Frequency Comb at 2.8-4.8 μm . *Opt Lett* **2009**, *34*, 1330-1332.

- 1
2
3 17. Meek, S.; Poisson, A.; Guelachvili, G.; Hänsch, T. W.; Picqué, N., Fourier
4 Transform Spectroscopy Around 3 μm with a Broad Difference Frequency Comb. *Appl*
5 *Phys B* **2014**, *114*, 573-578.
- 6 18. Lee, K. F.; Hensley, C. J.; Schunemann, P. G.; Fermann, M. E., Midinfrared
7 Frequency Comb by Difference Frequency of Erbium and Thulium Fiber Lasers in
8 Orientation-Patterned Gallium Phosphide. *Opt Express* **2017**, *25*, 17411-17416.
- 9 19. Iwakuni, K.; Porat, G.; Bui, T. Q.; Bjork, B. J.; Schoun, S. B.; Heckl, O. H.;
10 Fermann, M. E.; Ye, J., Phase-Stabilized 100 mW Frequency Comb Near 10 μm . *Appl*
11 *Phys B* **2018**, *124*, 128.
- 12 20. Muraviev, A. V.; Smolski, V. O.; Loparo, Z. E.; Vodopyanov, K. L., Massively
13 Parallel Sensing of Trace Molecules and Their Isotopologues with Broadband
14 Subharmonic Mid-Infrared Frequency Combs. *Nat Photonics* **2018**, *12*, 209-214.
- 15 21. Timmers, H.; Kowligy, A.; Lind, A.; Cruz, F. C.; Nader, N.; Silfies, M.; Yeas, G.;
16 Allison, T. K.; Schunemann, P. G.; Papp, S. B.; Diddams, S. A., Molecular
17 Fingerprinting with Bright, Broadband Infrared Frequency Combs. *Optica* **2018**, *5*, 727-
18 732.
- 19 22. Chen, Y.; Silfies, M. C.; Kowzan, G.; Bautista, J. M.; Allison, T. K., Tunable
20 Visible Frequency Combs from a Yb-Fiber-Laser-Pumped Optical Parametric Oscillator.
21 *Appl Phys B* **2019**, *125*, 81.
- 22 23. Lesko, D. M. B.; Timmers, H.; Xing, S.; Kowligy, A.; Lind, A. J.; Diddams, S. A.,
23 A Six-Octave Optical Frequency Comb from a Scalable Few-Cycle Erbium Fibre Laser.
24 *Nat Photonics* **2021**, *15*, 281.
- 25 24. Pupeza, I.; Zhang, C.; Högnér, M.; Ye, J., Extreme-Ultraviolet Frequency Combs for
26 Precision Metrology and Attosecond Science. *Nat Photonics* **2021**, *15*, 175-186.
- 27 25. Kippenberg, T. J.; Holzwarth, R.; Diddams, S. A., Microresonator-Based Optical
28 Frequency Combs. *Science* **2011**, *332*, 555-559.
- 29 26. Herr, T.; Brasch, V.; Jost, J. D.; Wang, C. Y.; Kondratiev, N. M.; Gorodetsky, M.
30 L.; Kippenberg, T. J., Temporal Solitons in Optical Microresonators. *Nat Photonics* **2014**,
31 *8*, 145-152.
- 32 27. Brasch, V.; Lucas, E.; Jost, J. D.; Geiselmann, M.; Kippenberg, T. J., Self-
33 Referenced Photonic Chip Soliton Kerr Frequency Comb. *Light-Sci Appl* **2017**, *6*,
34 e16202.
- 35 28. Suh, M.-G.; Yang, Q.-F.; Yang, K. Y.; Yi, X.; Vahala, K. J., Microresonator Soliton
36 Dual-Comb Spectroscopy. *Science* **2016**, *354*, 600-603.
- 37 29. Parriaux, A.; Hammani, K.; Millot, G., Electro-Optic Frequency Combs. *Adv Opt*
38 *Photonics* **2020**, *12*, 223-287.
- 39 30. Carlson, D. R.; Hickstein, D. D.; Zhang, W.; Metcalf, A. J.; Quinlan, F.; Diddams,
40 S. A.; Papp, S. B., Ultrafast Electro-Optic Light with Subcycle Control. *Science* **2018**,
41 *361*, 1358-1362.
- 42 31. Kazakov, D.; Piccardo, M.; Wang, Y.; Chevalier, P.; Mansuripur, T. S.; Xie, F.;
43 Zah, C.-e.; Lascola, K.; Belyanin, A.; Capasso, F., Self-Starting Harmonic Frequency
44 Comb Generation in a Quantum Cascade Laser. *Nat Photonics* **2017**, *11*, 789-792.
- 45 32. Hillbrand, J.; Andrews, A. M.; Detz, H.; Strasser, G.; Schwarz, B., Coherent
46 Injection Locking of Quantum Cascade Laser Frequency Combs. *Nat Photonics* **2019**, *13*,
47 101-104.
- 48 33. Villares, G.; Hugi, A.; Blaser, S.; Faist, J., Dual-Comb Spectroscopy Based on
49 Quantum-Cascade-Laser Frequency Combs. *Nat Commun* **2014**, *5*, 5192.
- 50 34. Sterczewski, L. A.; Westberg, J.; Bagheri, M.; Frez, C.; Vurgaftman, I.; Canedy,
51 C. L.; Bewley, W. W.; Merritt, C. D.; Kim, C. S.; Kim, M.; Meyer, J. R.; Wysocki, G.,
52
53

- 1
2
3 Mid-Infrared Dual-Comb Spectroscopy with Interband Cascade Lasers. *Opt Lett* **2019**,
4 *44*, 2113-2116.
- 5 35. Thorpe, M. J.; Balslev-Clausen, D.; Kirchner, M. S.; Ye, J., Cavity-Enhanced
6 Optical Frequency Comb Spectroscopy: Application to Human Breath Analysis. *Opt*
7 *Express* **2008**, *16*, 2387-2397.
- 8 36. Masłowski, P.; Cossel, K. C.; Foltynowicz, A.; Ye, J., Cavity-Enhanced Direct
9 Frequency Comb Spectroscopy. In *Cavity-Enhanced Spectroscopy and Sensing*,
10 Gagliardi, G.; Loock, H.-P., Eds. Springer: Berlin, Heidelberg, 2014; pp 271-321.
- 11 37. Mandon, J.; Guelachvili, G.; Picqué, N., Fourier Transform Spectroscopy with a
12 Laser Frequency Comb. *Nat Photonics* **2009**, *3*, 99-102.
- 13 38. Foltynowicz, A.; Ban, T.; Masłowski, P.; Adler, F.; Ye, J., Quantum-Noise-Limited
14 Optical Frequency Comb Spectroscopy. *Phys Rev Lett* **2011**, *107*, 233002.
- 15 39. Masłowski, P.; Lee, K. F.; Johansson, A. C.; Khodabakhsh, A.; Kowzan, G.;
16 Rutkowski, L.; Mills, A. A.; Mohr, C.; Jiang, J.; Fermann, M. E.; Foltynowicz, A.,
17 Surpassing the Path-Limited Resolution of Fourier-Transform Spectrometry with
18 Frequency Combs. *Phys Rev A* **2016**, *93*, 021802.
- 19 40. Coddington, I.; Newbury, N.; Swann, W., Dual-Comb Spectroscopy. *Optica* **2016**, *3*,
20 414-426.
- 21 41. Long, D. A.; Fleisher, A. J.; Douglass, K. O.; Maxwell, S. E.; Bielska, K.; Hodges,
22 J. T.; Plusquellic, D. F., Multiheterodyne Spectroscopy with Optical Frequency Combs
23 Generated from a Continuous-Wave Laser. *Opt Lett* **2014**, *39*, 2688-2690.
- 24 42. Fleisher, A. J.; Long, D. A.; Reed, Z. D.; Hodges, J. T.; Plusquellic, D. F., Coherent
25 Cavity-Enhanced Dual-Comb Spectroscopy. *Opt Express* **2016**, *24*, 10424-10434.
- 26 43. Znakovskaya, I.; Fill, E.; Forget, N.; Tournois, P.; Seidel, M.; Pronin, O.; Krausz,
27 F.; Apolonski, A., Dual Frequency Comb Spectroscopy with a Single Laser. *Opt Lett*
28 **2014**, *39*, 5471-5474.
- 29 44. Carlson, D. R.; Hickstein, D. D.; Cole, D. C.; Diddams, S. A.; Papp, S. B., Dual-
30 Comb Interferometry via Repetition Rate Switching of a Single Frequency Comb. *Opt*
31 *Lett* **2018**, *43*, 3614-3617.
- 32 45. Fellingner, J.; Mayer, A. S.; Winkler, G.; Grosinger, W.; Truong, G.-W.; Droste, S.;
33 Li, C.; Heyl, C. M.; Hartl, I.; Heckl, O. H., Tunable Dual-Comb from an All-
34 Polarization-Maintaining Single-Cavity Dual-Color Yb: fiber Laser. *Opt Express* **2019**,
35 *27*, 28062-28074.
- 36 46. Liao, R.; Tian, H.; Liu, W.; Li, R.; Song, Y.; Hu, M., Dual-Comb Generation from
37 a Single Laser Source: Principles and Spectroscopic Applications Towards Mid-IR: A
38 Review. *J Phys-Photonics* **2020**, *2*, 042006.
- 39 47. Roy, J.; Deschênes, J. D.; Potvin, S.; Genest, J., Continuous Real-Time Correction
40 and Averaging for Frequency Comb Interferometry. *Opt Express* **2012**, *20*, 21932-21939.
- 41 48. Deschênes, J. D.; Genest, J., Frequency-Noise Removal and On-Line Calibration for
42 Accurate Frequency Comb Interference Spectroscopy of Acetylene. *Appl Optics* **2014**,
43 *53*, 731-735.
- 44 49. Ideguchi, T.; Poisson, A.; Guelachvili, G.; Picqué, N.; Hänsch, T. W., Adaptive
45 Real-Time Dual-Comb Spectroscopy. *Nat Commun* **2014**, *5*, 3375.
- 46 50. Sterczewski, L. A.; Westberg, J.; Wysocki, G., Computational Coherent Averaging
47 for Free-Running Dual-Comb Spectroscopy. *Opt Express* **2019**, *27*, 23875-23893.
- 48 51. Sterczewski, L. A.; Przewłoka, A.; Kaszub, W.; Sotor, J., Computational Doppler-
49 Limited Dual-Comb Spectroscopy with a Free-Running All-Fiber Laser. *Appl Photonics*
50 **2019**, *4*, 116102.
- 51 52. Nugent-Glandorf, L.; Neely, T.; Adler, F.; Fleisher, A. J.; Cossel, K. C.; Bjork, B.;
52 Dinneen, T.; Ye, J.; Diddams, S. A., Mid-Infrared Virtually Imaged Phased Array

- 1
2
3 Spectrometer for Rapid and Broadband Trace Gas Detection. *Opt Lett* **2012**, *37*, 3285-
4 3287.
- 5 53. Iwakuni, K.; Bui, T. Q.; Niedermeyer, J. F.; Sukegawa, T.; Ye, J., Comb-Resolved
6 Spectroscopy with Immersion Grating in Long-Wave Infrared. *Opt Express* **2019**, *27*,
7 1911-1921.
- 8 54. Diddams, S. A.; Hollberg, L.; Mbele, V., Molecular Fingerprinting with the Resolved
9 Modes of a Femtosecond Laser Frequency Comb. *Nature* **2007**, *445*, 627-630.
- 10 55. Karim, F.; Scholten, S. K.; Perrella, C.; Luiten, A. N., Ultrahigh-Resolution Direct-
11 Frequency-Comb Spectrometer. *Phys Rev Appl* **2020**, *14*, 8.
- 12 56. Bjork, B. J.; Bui, T. Q.; Heckl, O. H.; Changala, P. B.; Spaun, B.; Heu, P.;
13 Follman, D.; Deutsch, C.; Cole, G. D.; Aspelmeyer, M.; Okumura, M.; Ye, J., Direct
14 Frequency Comb Measurement of OD + CO → DOCO Kinetics. *Science* **2016**, *354*, 444-
15 448.
- 16 57. Bailey, D. M.; Zhao, G.; Fleisher, A. J., Precision Spectroscopy of Nitrous Oxide
17 Isotopocules with a Cross-Dispersed Spectrometer and a Mid-Infrared Frequency Comb.
18 *Anal Chem* **2020**, *92*, 13759-13766.
- 19 58. Roberts, F. C.; Lewandowski, H. J.; Hobson, B. F.; Lehman, J. H., A Rapid,
20 Spatially Dispersive Frequency Comb Spectrograph Aimed at Gas Phase Chemical
21 Reaction Kinetics. *Mol Phys* **2020**, *118*, e1733116.
- 22 59. Finneran, I. A.; Good, J. T.; Holland, D. B.; Carroll, P. B.; Allodi, M. A.; Blake, G.
23 A., Decade-Spanning High-Precision Terahertz Frequency Comb. *Phys Rev Lett* **2015**,
24 *114*, 163902.
- 25 60. Kowligy, A. S.; Timmers, H.; Lind, A. J.; Elu, U.; Cruz, F. C.; Schunemann, P. G.;
26 Biegert, J.; Diddams, S. A., Infrared Electric Field Sampled Frequency Comb
27 Spectroscopy. *Sci Adv* **2019**, *5*, eaaw8794.
- 28 61. Gohle, C.; Stein, B.; Schliesser, A.; Udem, T.; Hänsch, T. W., Frequency Comb
29 Vernier Spectroscopy for Broadband, High-Resolution, High-Sensitivity Absorption and
30 Dispersion Spectra. *Phys Rev Lett* **2007**, *99*, 263902.
- 31 62. Khodabakhsh, A.; Ramaiah-Badarla, V.; Rutkowski, L.; Johansson, A. C.; Lee, K.
32 F.; Jiang, J.; Mohr, C.; Fermann, M. E.; Foltynowicz, A., Fourier Transform and
33 Vernier Spectroscopy using an Optical Frequency Comb at 3-5.4 μm. *Opt Lett* **2016**, *41*,
34 2541-2544.
- 35 63. Sadiq, I.; Mikkonen, T.; Vainio, M.; Toivonen, J.; Foltynowicz, A., Optical
36 Frequency Comb Photoacoustic Spectroscopy. *Phys Chem Chem Phys* **2018**, *20*, 27849-
37 27855.
- 38 64. Friedlein, J. T.; Baumann, E.; Briggman, K. A.; Colacion, G. M.; Giorgetta, F. R.;
39 Goldfain, A. M.; Herman, D. I.; Hoenig, E. V.; Hwang, J.; Newbury, N. R.; Perez, E.
40 F.; Yung, C. S.; Coddington, I.; Cossel, K. C., Dual-Comb Photoacoustic Spectroscopy.
41 *Nat Commun* **2020**, *11*, 10.
- 42 65. Wildi, T.; Voumard, T.; Brasch, V.; Yilmaz, G.; Herr, T., Photo-Acoustic Dual-
43 Frequency Comb Spectroscopy. *Nat Commun* **2020**, *11*, 4164.
- 44 66. Reber, M. A. R.; Chen, Y.; Allison, T. K., Cavity-Enhanced Ultrafast Spectroscopy:
45 Ultrafast Meets Ultrasensitive. *Optica* **2016**, *3*, 311-317.
- 46 67. Morgenweg, J.; Barmes, I.; Eikema, K. S. E., Ramsey-Comb Spectroscopy with
47 Intense Ultrashort Laser Pulses. *Nat Phys* **2014**, *10*, 30-33.
- 48 68. Ding, S.; Matsukevich, D. N., Quantum Logic for the Control and Manipulation of
49 Molecular Ions using a Frequency Comb. *New J Phys* **2012**, *14*, 023028.
- 50 69. Chou, C. W.; Collopy, A. L.; Kurz, C.; Lin, Y.; Harding, M. E.; Plessow, P. N.;
51 Fortier, T.; Diddams, S.; Leibfried, D.; Leibbrandt, D. R., Frequency-Comb Spectroscopy
52 on Pure Quantum States of a Single Molecular Ion. *Science* **2020**, *367*, 1458-1461.
- 53
54
55
56

- 1
2
3 70. Hébert, N. B.; Scholten, S. K.; White, R. T.; Genest, J.; Luiten, A. N.; Anstie, J. D.,
4 A Quantitative Mode-Resolved Frequency Comb Spectrometer. *Opt Express* **2015**, *23*,
5 13991-14001.
- 6 71. Spaun, B.; Changala, P. B.; Patterson, D.; Bjork, B. J.; Heckl, O. H.; Doyle, J. M.;
7 Ye, J., Continuous Probing of Cold Complex Molecules with Infrared Frequency Comb
8 Spectroscopy. *Nature* **2016**, *533*, 517-520.
- 9 72. Changala, P. B.; Spaun, B.; Patterson, D.; Doyle, J. M.; Ye, J., Sensitivity and
10 Resolution in Frequency Comb Spectroscopy of Buffer Gas Cooled Polyatomic
11 Molecules. *Appl Phys B* **2016**, *122*, 292.
- 12 73. *Cavity-Enhanced Spectroscopy and Sensing*. Springer: 2014.
- 13 74. Changala, P. B.; Weichman, M. L.; Lee, K. F.; Fermann, M. E.; Ye, J.,
14 Rovibrational Quantum State Resolution of the C₆₀ Fullerene. *Science* **2019**, *363*, 49-54.
- 15 75. Berera, R.; van Grondelle, R.; Kennis, J. T. M., Ultrafast Transient Absorption
16 Spectroscopy: Principles and Application to Photosynthetic Systems. *Photosynth Res*
17 **2009**, *101*, 105-118.
- 18 76. Schrieffer, C.; Lochbrunner, S.; Riedle, E.; Nesbitt, D. J., Ultrasensitive Ultraviolet-
19 Visible 20 fs Absorption Spectroscopy of Low Vapor Pressure Molecules in the Gas
20 Phase. *Rev Sci Instrum* **2008**, *79*, 013107.
- 21 77. Silfies, M. C.; Kowzan, G.; Chen, Y. N.; Lewis, N.; Hou, R.; Baehre, R.; Gross,
22 T.; Allison, T. K., Widely Tunable Cavity-Enhanced Frequency Combs. *Opt Lett* **2020**,
23 *45*, 2123-2126.
- 24 78. Silfies, M. C.; Kowzan, G.; Lewis, N.; Allison, T. K., Broadband Cavity-Enhanced
25 Ultrafast Spectroscopy. *Phys Chem Chem Phys* **2021**, *23*, 9743-9752.
- 26 79. Lomsadze, B.; Cundiff, S. T., Frequency Combs Enable Rapid and High-Resolution
27 Multidimensional Coherent Spectroscopy. *Science* **2017**, *357*, 1389-1391.
- 28 80. Lomsadze, B.; Smith, B. C.; Cundiff, S. T., Tri-comb spectroscopy. *Nat Photonics*
29 **2018**, *12*, 676-680.
- 30 81. Allison, T. K., Cavity-Enhanced Ultrafast Two-Dimensional Spectroscopy Using
31 Higher Order Modes. *J Phys B-at Mol Opt* **2017**, *50*, 044004.
- 32 82. Snow, T. P.; Bierbaum, V. M., Ion Chemistry in the Interstellar Medium. *Annu Rev*
33 *Anal Chem* **2008**, *1*, 229-259.
- 34 83. McGuire, B. A.; Asvany, O.; Brünken, S.; Schlemmer, S., Laboratory Spectroscopy
35 Techniques to Enable Observations of Interstellar Ion Chemistry. *Nat Rev Phys* **2020**, *2*,
36 402-410.
- 37 84. Puri, P.; Mills, M.; Schneider, C.; Simbotin, I.; Montgomery, J. A.; Cote, R.;
38 Suits, A. G.; Hudson, E. R., Synthesis of Mixed Hypermetallic Oxide BaOCa⁺ from
39 Laser-Cooled Reagents in an Atom-Ion Hybrid Trap. *Science* **2017**, *357*, 1370-+.
- 40 85. Cairncross, W. B.; Gresh, D. N.; Grau, M.; Cossel, K. C.; Roussy, T. S.; Ni, Y.;
41 Zhou, Y.; Ye, J.; Cornell, E. A., Precision Measurement of the Electron's Electric Dipole
42 Moment using Trapped Molecular Ions. *Phys Rev Lett* **2017**, *119*, 153001.
- 43 86. Chou, C.-W.; Kurz, C.; Hume, D. B.; Plessow, P. N.; Leibbrandt, D. R.; Leibfried,
44 D., Preparation and Coherent Manipulation of Pure Quantum States of a Single
45 Molecular Ion. *Nature* **2017**, *545*, 203-+.
- 46 87. Asvany, O.; Krieg, J.; Schlemmer, S., Frequency Comb Assisted Mid-Infrared
47 Spectroscopy of Cold Molecular Ions. *Rev Sci Instrum* **2012**, *83*, 093110.
- 48 88. Jusko, P.; Konietzko, C.; Schlemmer, S.; Asvany, O., Frequency Comb Assisted
49 Measurement of Fundamental Transitions of Cold H₃⁺, H₂D⁺ and D₂H⁺. *J Mol Spectrosc*
50 **2016**, *319*, 55-58.

- 1
2
3 89. Asvany, O.; Yamada, K. M. T.; Brünken, S.; Potapov, A.; Schlemmer, S.,
4 Experimental Ground-State Combination Differences of CH₅⁺. *Science* **2015**, *347*, 1346-
5 1349.
- 6 90. Markus, C. R.; McCall, B. J., Highly Accurate Experimentally Determined Energy
7 Levels of H₃⁺. *J Chem Phys* **2019**, *150*, 214303.
- 8 91. Sinclair, L. C.; Cossel, K. C.; Coffey, T.; Ye, J.; Cornell, E. A., Frequency Comb
9 Velocity-Modulation Spectroscopy. *Phys Rev Lett* **2011**, *107*, 093002.
- 10 92. Gresh, D. N.; Cossel, K. C.; Zhou, Y.; Ye, J.; Cornell, E. A., Broadband Velocity
11 Modulation Spectroscopy of ThF⁺ for Use in a Measurement of the Electron Electric
12 Dipole Moment. *J Mol Spectrosc* **2016**, *319*, 1-9.
- 13 93. Foltynowicz, A.; Rutkowski, L.; Silander, I.; Johansson, A. C.; de Oliveira, V. S.;
14 Axner, O.; Soboń, G.; Martynkien, T.; Mergo, P.; Lehmann, K. K., Sub-Doppler
15 Double-Resonance Spectroscopy of Methane using a Frequency Comb Probe. *Phys Rev*
16 *Lett* **2021**, *126*, 063001.
- 17 94. Foltynowicz, A.; Rutkowski, L.; Silander, I.; Johansson, A. C.; de Oliveira, V. S.;
18 Axner, O.; Soboń, G.; Martynkien, T.; Mergo, P.; Lehmann, K. K., Measurement and
19 Assignment of Double-Resonance Transitions to the 8900-9100-cm⁻¹ Levels of Methane.
20 *Phys Rev A* **2021**, *103*, 022810.
- 21 95. Hargreaves, R. J.; Gordon, I. E.; Rey, M.; Nikitin, A. V.; Tyuterev, V. G.;
22 Kochanov, R. V.; Rothman, L. S., An Accurate, Extensive, and Practical Line List of
23 Methane for the HITEMP Database. *Astrophys J Suppl S* **2020**, *247*, 55.
- 24 96. Kocheril, P. A.; Markus, C. R.; Esposito, A. M.; Schrader, A. W.; Dieter, T. S.;
25 McCall, B. J., Extended Sub-Doppler Resolution Spectroscopy of the ν₃ Band of
26 Methane. *J Quant Spectrosc Radiat Transf* **2018**, *215*, 9-12.
- 27 97. Hu, C. L.; Perevalov, V. I.; Cheng, C. F.; Hua, T.-P.; Liu, A.-W.; Sun, Y. R.; Tan,
28 Y.; Wang, J.; Hu, S.-M., Optical-Optical Double-Resonance Absorption Spectroscopy of
29 Molecules with Kilohertz Accuracy. *J Phys Chem Lett* **2020**, *11*, 7843-7848.
- 30 98. Okubo, S.; Inaba, H.; Okuda, S.; Sasada, H., Frequency Measurements of the 2ν₃
31 A₁-ν₃ Band Transitions of Methane in Comb-Referenced Infrared-Infrared Double-
32 Resonance Spectroscopy. *Phys Rev A* **2021**, *103*, 022809.
- 33 99. Long, D. A.; Fleisher, A. J.; Plusquellic, D. F.; Hodges, J. T., Multiplexed Sub-
34 Doppler Spectroscopy with an Optical Frequency Comb. *Phys Rev A* **2016**, *94*, 061801.
- 35 100. Chevalier, M.; De Martino, A., Double-Resonance Observation of the (3ν₃, F₁) State
36 of Methane. *Chem Phys Lett* **1987**, *135*, 446-450.
- 37 101. Bañares, M. A.; Guerrero-Pérez, M. O.; Fierro, J. L. G.; Cortez, G. G., Raman
38 Spectroscopy during Catalytic Operations with On-Line Activity Measurement
39 (Operando Spectroscopy): A Method for Understanding the Active Centres of Cations
40 Supported on Porous Materials. *J Mater Chem* **2002**, *12*, 3337-3342.
- 41 102. Kohse-Höinghaus, K.; Troe, J.; Grabow, J.-U.; Olzmann, M.; Friedrichs, G.;
42 Hungenberg, K.-D., Kinetics in the Real World: Linking Molecules, Processes, and
43 Systems. *Phys Chem Chem Phys* **2018**, *20*, 10561-10568.
- 44 103. Bui, T. Q.; Bjork, B. J.; Changala, P. B.; Heckl, O. H.; Spaun, B.; Ye, J.,
45 OD+CO→D+CO₂ Branching Kinetics Probed with Time-Resolved Frequency Comb
46 Spectroscopy. *Chem Phys Lett* **2017**, *683*, 91-95.
- 47 104. Bui, T. Q.; Bjork, B. J.; Changala, P. B.; Nguyen, T. L.; Stanton, J. F.; Okumura,
48 M.; Ye, J., Direct Measurements of DOCO Isomers in the Kinetics of OD + CO. *Sci Adv*
49 **2018**, *4*, eaao4777.
- 50 105. Bui, T. Q.; Changala, P. B.; Bjork, B. J.; Yu, Q.; Wang, Y.; Stanton, J. F.;
51 Bowman, J.; Ye, J., Spectral Analyses of *trans*- and *cis*-DOCO Transients via Comb
52 Spectroscopy. *Mol Phys* **2018**, *116*, 3710-3717.

- 1
2
3 106. Lins, E.; Read, S.; Unni, B.; Rosendahl, S. M.; Burgess, I. J., Microsecond
4 Resolved Infrared Spectroelectrochemistry Using Dual Frequency Comb IR Lasers. *Anal*
5 *Chem* **2020**, *92*, 6241-6244.
- 6 107. Norahan, M. J.; Horvath, R.; Woitzik, N.; Jouy, P.; Eigenmann, F.; Gerwert, K.;
7 Kötting, C., Microsecond-Resolved Infrared Spectroscopy on Nonrepetitive Protein
8 Reactions by Applying Caged Compounds and Quantum Cascade Laser Frequency
9 Combs. *Anal Chem* **2021**, *93*, 6779-6783.
- 10 108. Fleisher, A. J.; Bjork, B. J.; Bui, T. Q.; Cossel, K. C.; Okumura, M.; Ye, J., Mid-
11 Infrared Time-Resolved Frequency Comb Spectroscopy of Transient Free Radicals. *J*
12 *Phys Chem Lett* **2014**, *5*, 2241-2246.
- 13 109. Rockmore, R.; Gibson, R.; Moloney, J. V.; Jones, R. J., VECSEL-Based Virtually
14 Imaged Phased Array Spectrometer for Rapid Gas Phase Detection in the Mid-Infrared.
15 *Opt Lett* **2020**, *45*, 5796-5799.
- 16 110. Luo, P. L.; Horng, E. C., Simultaneous Determination of Transient Free Radicals
17 and Reaction Kinetics by High-Resolution Time-Resolved Dual-Comb Spectroscopy.
18 *Comm Chem* **2020**, *3*, 8.
- 19 111. Luo, P. L., Long-Wave Mid-Infrared Time-Resolved Dual-Comb Spectroscopy of
20 Short-Lived Intermediates. *Opt Lett* **2020**, *45*, 6791-6794.
- 21 112. Luo, P. L.; Horng, E. C.; Guan, Y. C., Fast Molecular Fingerprinting with a
22 Coherent, Rapidly Tunable Dual-Comb Spectrometer near 3 μm . *Phys Chem Chem Phys*
23 **2019**, *21*, 18400-18405.
- 24 113. Sterczewski, L. A.; Westberg, J.; Yang, Y.; Burghoff, D.; Reno, J.; Hu, Q.;
25 Wysocki, G., Terahertz Spectroscopy of Gas Mixtures with Dual Quantum Cascade Laser
26 Frequency Combs. *ACS Photonics* **2020**, *7*, 1082-1087.
- 27 114. Abbas, M. A.; Pan, Q.; Mandon, J.; Cristescu, S. M.; Harren, F. J. M.;
28 Khodabakhsh, A., Time-Resolved Mid-Infrared Dual-Comb Spectroscopy. *Sci Rep* **2019**,
29 *9*, 9.
- 30 115. Fjodorow, P.; Allmendinger, P.; Horvath, R.; Herzler, J.; Eigenmann, F.; Geiser,
31 M.; Fikri, M.; Schulz, C., Monitoring Formaldehyde in a Shock Tube with a Fast Dual-
32 Comb Spectrometer Operating in the Spectral Range of 1740-1790 cm^{-1} . *Appl Phys B*
33 **2020**, *126*, 11.
- 34 116. Hayden, T. R. S.; Malarich, N.; Petrykowski, D.; Nigam, S. P.; Christopher, J. D.;
35 Lapointe, C.; Wimer, N. T.; Hamlington, P. E.; Rieker, G. B., OH Radical
36 Measurements in Combustion Environments using Wavelength Modulation Spectroscopy
37 and Dual-Frequency Comb Spectroscopy Near 1491 nm. *Appl Phys B* **2019**, *125*, 14.
- 38 117. Pinkowski, N. H.; Cassidy, S. J.; Strand, C. L.; Hanson, R. K., Quantum-Cascade-
39 Laser-Based Dual-Comb Thermometry and Speciation at High Temperatures. *Meas Sci*
40 *Technol* **2021**, *32*, 16.
- 41 118. Zhang, G. L.; Horvath, R.; Liu, D. P.; Geiser, M.; Farooq, A., QCL-Based Dual-
42 Comb Spectrometer for Multi-Species Measurements at High Temperatures and High
43 Pressures. *Sensors* **2020**, *20*, 14.
- 44 119. Abbas, M. A.; van Dijk, L.; Jahromi, K. E.; Nematollahi, M.; Harren, F. J. M.;
45 Khodabakhsh, A., Broadband Time-Resolved Absorption and Dispersion Spectroscopy
46 of Methane and Ethane in a Plasma Using a Mid-Infrared Dual-Comb Spectrometer.
47 *Sensors* **2020**, *20*, 25.
- 48 120. Hoghooghi, N.; Cole, R. K.; Rieker, G. B., 11- μs time-resolved, continuous dual-
49 comb spectroscopy with spectrally filtered mode-locked frequency combs. *Appl Phys B*
50 **2021**, *127*, 10.

- 1
2
3 121. Zhang, Y.; Weeks, R. R. D.; Lecaplain, C.; Harilal, S. S.; Yeak, J.; Phillips, M.
4 C.; Jones, R. J., Burst-Mode Dual-Comb Spectroscopy. *Opt Lett* **2021**, *46*, 860-863.
5 122. Xu, K.; Ma, L. H.; Chen, J.; Zhao, X.; Wang, Q.; Kan, R. F.; Zheng, Z.; Ren,
6 W., Dual-Comb Spectroscopy for Laminar Premixed Flames with a Free-running Fiber
7 Laser. *Combust Sci Technol* **2021**, DOI:10.1080/00102202.2021.1879796.
8 123. Khan, M. A. H.; Percival, C. J.; Caravan, R. L.; Taatjes, C. A.; Shallcross, D. E.,
9 Criegee Intermediates and Their Impacts on the Troposphere. *Environ Sci-Process*
10 *Impacts* **2018**, *20*, 437-453.
11 124. Welz, O.; Savee, J. D.; Osborn, D. L.; Vasu, S. S.; Percival, C. J.; Shallcross, D.
12 E.; Taatjes, C. A., Direct Kinetic Measurements of Criegee Intermediate (CH₂OO)
13 Formed by Reaction of CH₂I with O₂. *Science* **2012**, *335*, 204-207.
14 125. Chhantyal-Pun, R.; Khan, M. A. H.; Taatjes, C. A.; Percival, C. J.; Orr-Ewing, A.
15 J.; Shallcross, D. E., Criegee Intermediates: Production, Detection and Reactivity. *Int Rev*
16 *Phys Chem* **2020**, *39*, 385-424.
17 126. Luo, P.-L.; Endo, Y.; Lee, Y.-P., Identification and Self-Reaction Kinetics of
18 Criegee Intermediates *syn*-CH₃CHO and CH₂OO via High-Resolution Infrared Spectra
19 with a Quantum-Cascade Laser. *J Phys Chem Lett* **2018**, *9*, 4391-4395.
20 127. Chang, Y.-P.; Merer, A. J.; Chang, H.-H.; Jhang, L.-J.; Chao, W.; Lin, J. J.-M.,
21 High Resolution Quantum Cascade Laser Spectroscopy of the Simplest Criegee
22 Intermediate, CH₂OO, between 1273 cm⁻¹ and 1290 cm⁻¹. *J Chem Phys* **2017**, *146*,
23 244302.
24 128. Su, Y.-T.; Huang, Y.-H.; Witek, H. A.; Lee, Y.-P., Infrared Absorption Spectrum
25 of the Simplest Criegee Intermediate CH₂OO. *Science* **2013**, *340*, 174-176.
26 129. Huang, Y.-H.; Li, J.; Guo, H.; Lee, Y.-P., Infrared Spectrum of the Simplest
27 Criegee Intermediate CH₂OO at Resolution 0.25 cm⁻¹ and New Assignments of Bands
28 2ν₉ and ν₅. *J Chem Phys* **2015**, *142*, 214301.
29 130. Gordon, I. E.; Rothman, L. S.; Hill, C.; Kochanov, R. V.; Tan, Y.; Bernath, P. F.;
30 Birk, M.; Boudon, V.; Campargue, A.; Chance, K. V.; Drouin, B. J.; Flaud, J. M.;
31 Gamache, R. R.; Hodges, J. T.; Jacquemart, D.; Perevalov, V. I.; Perrin, A.; Shine, K.
32 P.; Smith, M. A. H.; Tennyson, J.; Toon, G. C.; Tran, H.; Tyuterev, V. G.; Barbe, A.;
33 Császár, A. G.; Devi, V. M.; Furtenbacher, T.; Harrison, J. J.; Hartmann, J. M.; Jolly,
34 A.; Johnson, T. J.; Karman, T.; Kleiner, I.; Kyuberis, A. A.; Loos, J.; Lyulin, O. M.;
35 Massie, S. T.; Mikhailenko, S. N.; Moazzen-Ahmadi, N.; Müller, H. S. P.; Naumenko,
36 O. V.; Nikitin, A. V.; Polyansky, O. L.; Rey, M.; Rotger, M.; Sharpe, S. W.; Sung,
37 K.; Starikova, E.; Tashkun, S. A.; Auwera, J. V.; Wagner, G.; Wilzewski, J.; Wcisło,
38 P.; Yu, S.; Zak, E. J., The HITRAN2016 Molecular Spectroscopic Database. *J Quant*
39 *Spectrosc Radiat Transf* **2017**, *203*, 3-69.
40 131. Ideguchi, T.; Holzner, S.; Bernhardt, B.; Guelachvili, G.; Picqué, N.; Hänsch, T.
41 W., Coherent Raman Spectro-Imaging with Laser Frequency Combs. *Nature* **2013**, *502*,
42 355-358.
43 132. Coluccelli, N.; Howle, C. R.; McEwan, K.; Wang, Y.; Fernandez, T. T.;
44 Gambetta, A.; Laporta, P.; Galzerano, G., Fiber-Format Dual-Comb Coherent Raman
45 Spectrometer. *Opt Lett* **2017**, *42*, 4683-4686.
46 133. Herman, D. I.; Waxman, E. M.; Ycas, G.; Giorgetta, F. R.; Newbury, N. R.;
47 Coddington, I. R., Real-Time Liquid-Phase Organic Reaction Monitoring with Mid-
48 Infrared Attenuated Total Reflectance Dual Frequency Comb Spectroscopy. *J Mol*
49 *Spectrosc* **2019**, *356*, 39-45.
50 134. Klocke, J. L.; Mangold, M.; Allmendinger, P.; Hugi, A.; Geiser, M.; Jouy, P.;
51 Faist, J.; Kottke, T., Single-Shot Sub-Microsecond Mid-Infrared Spectroscopy on Protein
52
53

- 1
2
3 Reactions with Quantum Cascade Laser Frequency Combs. *Anal Chem* **2018**, *90*, 10494-
4 10500.
- 5 135. Schnee, J.; Bazin, P.; Barviau, B.; Grisch, F.; Beccard, B. J.; Daturi, M., Coupling
6 a Rapid-Scan FT-IR Spectrometer with Quantum Cascade Lasers within a Single Setup:
7 An Easy Way to Reach Microsecond Time Resolution without Losing Spectral
8 Information. *Anal Chem* **2019**, *91*, 4368-4373.
- 9 136. Qin, Y.; Cromey, B.; Batjargal, O.; Kieu, K., All-Fiber Single-Cavity Dual-Comb
10 for Coherent Anti-Stokes Raman Scattering Spectroscopy Based on Spectral Focusing.
11 *Opt Lett* **2021**, *46*, 146-149.
- 12 137. Kameyama, R.; Takizawa, S.; Hiramatsu, K.; Goda, K., Dual-Comb Coherent
13 Raman Spectroscopy with near 100% Duty Cycle. *ACS Photonics* **2020**, *8*, 975.
- 14 138. Han, N. S.; Kim, J.; Yoon, T. H.; Cho, M., Broadband Infrared Spectroscopy of
15 Molecules in Solutions with Two Intrapulse Difference-Frequency-Generated Mid-
16 Infrared Frequency Combs. *J Phys Chem B* **2021**, *125*, 307-316.
- 17 139. Cho, Y. E.; Maeng, J. Y.; Kim, S.; Hong, S., Formation of Highly Ordered Organic
18 Monolayers by Dative Bonding: Pyridine on Ge(100). *J Am Chem Soc* **2003**, *125*, 7514-
19 7515.
- 20 140. Wolkow, R. A., Controlled Molecular Adsorption On Silicon: Laying a Foundation
21 for Molecular Devices. *Annu Rev Phys Chem* **1999**, *50*, 413-441.
- 22 141. Waxman, E. M.; Cossel, K. C.; Truong, G. W.; Giorgetta, F. R.; Swann, W. C.;
23 Coburn, S.; Wright, R. J.; Rieker, G. B.; Coddington, I.; Newbury, N. R.,
24 Intercomparison of Open-Path Trace Gas Measurements with Two Dual-Frequency-
25 Comb Spectrometers. *Atmos Meas Tech* **2017**, *10*, 3295-3311.
- 26 142. Ycas, G.; Giorgetta, F. R.; Cossel, K. C.; Waxman, E. M.; Baumann, E.;
27 Newbury, N. R.; Coddington, I., Mid-Infrared Dual-Comb Spectroscopy of Volatile
28 Organic Compounds Across Long Open-Air Paths. *Optica* **2019**, *6*, 165-168.
- 29 143. Ycas, G.; Giorgetta, F. R.; Friedlein, J. T.; Herman, D.; Cossel, K. C.; Baumann,
30 E.; Newbury, N. R.; Coddington, I., Compact Mid-Infrared Dual-Comb Spectrometer for
31 Outdoor Spectroscopy. *Opt Express* **2020**, *28*, 14740-14752.
- 32 144. Alden, C. B.; Wright, R. J.; Coburn, S. C.; Caputi, D.; Wendland, G.; Rybchuk,
33 A.; Conley, S.; Faloon, I.; Rieker, G. B., Temporal Variability of Emissions Revealed
34 by Continuous, Long-Term Monitoring of an Underground Natural Gas Storage Facility.
35 *Environ Sci Technol* **2020**, *54*, 14589-14597.
- 36 145. Makowiecki, A. S.; Steinbrenner, J. E.; Wimer, N. T.; Glusman, J. F.; Lapointe,
37 C. B.; Daily, J. W.; Hamlington, P. E.; Rieker, G. B., Dual Frequency Comb
38 Spectroscopy of Solid Fuel Pyrolysis and Combustion: Quantifying the Influence of
39 Moisture Content in Douglas Fir. *Fire Saf J* **2020**, *116*, 8.
- 40 146. Schliesser, A.; Brehm, M.; Keilmann, F.; van der Weide, D. W., Frequency-Comb
41 Infrared Spectrometer for Rapid, Remote Chemical Sensing. *Opt Express* **2005**, *13*, 9029-
42 9038.
- 43 147. Truong, G.-W.; Waxman, E. M.; Cossel, K. C.; Baumann, E.; Klose, A.;
44 Giorgetta, F. R.; Swann, W. C.; Newbury, N. R.; Coddington, I., Accurate Frequency
45 Referencing for Fieldable Dual-Comb Spectroscopy. *Opt Express* **2016**, *24*, 30495-
46 30504.
- 47 148. Cossel, K. C.; Waxman, E. M.; Giorgetta, F. R.; Cermak, M.; Coddington, I. R.;
48 Hesselius, D.; Ruben, S.; Swann, W. C.; Truong, G.-W.; Rieker, G. B.; Newbury, N.
49 R., Open-Path Dual-Comb Spectroscopy to an Airborne Retroreflector. *Optica* **2017**, *4*,
50 724-728.
- 51 149. Rieker, G. B.; Giorgetta, F. R.; Swann, W. C.; Kofler, J.; Zolot, A. M.; Sinclair,
52 L. C.; Baumann, E.; Cromer, C.; Petron, G.; Sweeney, C.; Tans, P. P.; Coddington, I.;

- 1
2
3 Newbury, N. R., Frequency-Comb-Based Remote Sensing of Greenhouse Gases over
4 Kilometer Air Paths. *Optica* **2014**, *1*, 290-298.
- 5 150. Yang, K.; Li, H.; Gong, H.; Shen, X.; Hao, Q.; Yan, M.; Huang, K.; Zeng, H.,
6 Temperature Measurement Based on Adaptive Dual-Comb Absorption Spectral
7 Detection. *Chin Opt Lett* **2020**, *18*, 051401.
- 8 151. Waxman, E. M.; Cossel, K. C.; Giorgetta, F.; Truong, G. W.; Swann, W. C.;
9 Coddington, I.; Newbury, N. R., Estimating Vehicle Carbon Dioxide Emissions from
10 Boulder, Colorado, Using Horizontal Path-Integrated Column Measurements. *Atmos*
11 *Chem Phys* **2019**, *19*, 4177-4192.
- 12 152. Shimizu, Y.; Okubo, S.; Onae, A.; Yamada, K. M. T.; Inaba, H. T., Molecular Gas
13 Thermometry on Acetylene using Dual-Comb Spectroscopy: Analysis of Rotational
14 Energy Distribution. *Appl Phys B* **2018**, *124*, 8.
- 15 153. Coburn, S.; Alden, C. B.; Wright, R.; Cossel, K.; Baumann, E.; Truong, G. W.;
16 Giorgetta, F.; Sweeney, C.; Newbury, N. R.; Prasad, K.; Coddington, I.; Rieker, G. B.,
17 Regional Trace-Gas Source Attribution Using a Field-Deployed Dual Frequency Comb
18 Spectrometer. *Optica* **2018**, *5*, 320-327.
- 19 154. Wang, C.; Sahay, P., Breath Analysis Using Laser Spectroscopic Techniques:
20 Breath Biomarkers, Spectral Fingerprints, and Detection Limits. *Sensors* **2009**, *9*, 8230-
21 8262.
- 22 155. Metsala, M., Optical Techniques for Breath Analysis: From Single to Multi-Species
23 Detection. *J Breath Res* **2018**, *12*, 027104.
- 24 156. Li, J. Y.; Yu, Z. W.; Du, Z. H.; Ji, Y.; Liu, C., Standoff Chemical Detection Using
25 Laser Absorption Spectroscopy: A Review. *Remote Sens* **2020**, *12*, 44.
- 26 157. Spinelle, L.; Gerboles, M.; Kok, G.; Persijn, S.; Sauerwald, T., Review of Portable
27 and Low-Cost Sensors for the Ambient Air Monitoring of Benzene and Other Volatile
28 Organic Compounds. *Sensors* **2017**, *17*, 30.
- 29 158. Abreu, P.; Carslaw, D.; Davies, T.; Demie, J.; Kent, A.; Stacey, B.; Telling, S.;
30 Wakeling, D., UK Hydrocarbons Network Annual Report for 2015, Defra (Department
31 for the Environment Food and Rural Affairs). Ricardo-AEA: 2016.
- 32 159. Chen, T.; Xue, L.; Zheng, P.; Zhang, Y.; Liu, Y.; Sun, J.; Han, G.; Li, H.;
33 Zhang, X.; Li, Y.; Li, H.; Dong, C.; Xu, F.; Zhang, Q.; Wang, W., Volatile Organic
34 Compounds and Ozone Air Pollution in an Oil Production Region in Northern China.
35 *Atmos Chem Phys* **2020**, *20*, 7069-7086.
- 36 160. Li, S.-M.; Leithead, A.; Moussa, S. G.; Liggio, J.; Moran, M. D.; Wang, D.;
37 Hayden, K.; Darlington, A.; Gordon, M.; Staebler, R.; Makar, P. A.; Stroud, C. A.;
38 McLaren, R.; Liu, P. S. K.; O'Brien, J.; Mittermeier, R. L.; Zhang, J.; Marson, G.;
39 Cober, S. G.; Wolde, M.; Wentzell, J. J. B., Differences Between Measured and
40 Reported Volatile Organic Compound Emissions from Oil Sands Facilities in Alberta,
41 Canada. *Proc Natl Acad Sci USA* **2017**, 201617862.
- 42 161. Cooke, I. R.; Sims, I. R., Experimental Studies of Gas-Phase Reactivity in Relation
43 to Complex Organic Molecules in Star-Forming Regions. *ACS Earth Space Chem* **2019**,
44 *3*, 1109-1134.
- 45 162. Yue, J.; Schouten, J. C.; Nijhuis, T. A., Integration of Microreactors with
46 Spectroscopic Detection for Online Reaction Monitoring and Catalyst Characterization.
47 *Ind Eng Chem Res* **2012**, *51*, 14583-14609.
- 48 163. Pereira, J.; Porto-Figueira, P.; Cavaco, C.; Taunk, K.; Rapole, S.; Dhakne, R.;
49 Nagarajaram, H.; Câmara, J. S., Breath Analysis as a Potential and Non-Invasive Frontier
50 in Disease Diagnosis: An Overview. *Metabolites* **2015**, *5*, 3-55.